**Table 3. Body and Tissue Weights of Mice After 11 Weeks on Study Diets in Experiment I**

| | | | | | Two-Way ANOVA *P* Value | | |
|---|---|---|---|---|---|---|---|
| | | St | Suc | Saf | Diet | Fish oil | Diet × Fish Oil |
| | Fish oil | | | | | | |
| n | − | 9 | 8 | 9 | | | |
| | + | 5 | 8 | 8 | | | |
| Weight (g) | | | | | | | |
| BW at start | − | 31.7 ± 0.6 | 31.3 ± 0.7 | 31.4 ± 0.7 | | | |
| | + | 31.2 ± 0.7 | 31.3 ± 0.7 | 31.3 ± 0.6 | | | |
| Final BW | − | 52.8 ± 2.6$^{a}$ | 56.2 ± 3.1$^{ab}$ | 61.6 ± 2.0$^{bc}$ | | | |
| | + | 51.9 ± 4.9$^{a}$ | 55.4 ± 1.3$^{ac}$ | 62.7 ± 1.5$^{b}$ | 0.002 | 0.944 | 0.904 |
| Liver | − | 1.94 ± 0.09$^{a}$ | 2.33 ± 0.18$^{b}$ | 2.48 ± 0.14$^{b}$ | | | |
| | + | 1.93 ± 0.17$^{a}$ | 2.17 ± 0.11$^{ab}$ | 3.07 ± 0.06$^{c}$ | <0.001 | 0.203 | 0.011 |
| Epididymal WAT | − | 2.10 ± 0.29$^{abc}$ | 2.33 ± 0.27$^{cde}$ | 2.80 ± 0.19$^{e}$ | | | |
| | + | 1.52 ± 0.30$^{a}$ | 1.84 ± 0.14$^{abd}$ | 2.30 ± 0.14$^{be}$ | 0.012 | 0.010 | 0.983 |
| Retroperitoneal WAT | − | 0.43 ± 0.05 | 0.50 ± 0.07 | 0.48 ± 0.05 | | | |
| | + | 0.36 ± 0.06 | 0.40 ± 0.03 | 0.43 ± 0.02 | 0.385 | 0.068 | 0.869 |
| Mesenteric WAT | − | 1.39 ± 0.46 | 1.46 ± 0.29 | 1.57 ± 0.20 | | | |
| | + | 0.99 ± 0.27 | 1.02 ± 0.11 | 1.47 ± 0.09 | 0.404 | 0.165 | 0.789 |
| Subcutaneous WAT | − | 1.45 ± 0.21$^{ab}$ | 1.49 ± 0.26$^{ab}$ | 1.85 ± 0.16$^{b}$ | | | |
| | + | 0.95 ± 0.34$^{a}$ | 1.52 ± 0.11$^{ab}$ | 1.96 ± 0.21$^{b}$ | 0.009 | 0.503 | 0.344 |

Abbreviations: St, high-starch diet; Suc, high-starch diet with 20% (w/w) sucrose drink; Saf, high-safflower oil diet; BW, body weight; WAT, white adipose tissue. Values are mean ± SEM. Means without a common letter differ ($P < 0.05$).

regulator of lipogenesis in the liver.[14] SREBP-1a is less abundant in the liver but is more potent in fatty acid synthesis than SREBP-1c.[15] To examine whether the increased hepatic TG content in sucrose-supplemented mice was caused by activation of SREBP-1 (relative to that in high-starch–fed mice), mRNAs for SREPB-1 and the lipogenic enzymes fatty acid synthase (FAS), stearoyl-CoA desaturase 1 (SCD1), and acetyl-CoA carboxylase 1 (ACC1) were measured by quantitative reverse transcription PCR (Fig. 5). Sucrose-supplementation resulted in a 2.2-fold increase in SREBP-1c mRNA but did not affect SREBP-1a mRNA, compared with high-starch–fed mice. FAS and ACC1 mRNAs, but not SCD1 mRNA, were also increased in sucrose-supplemented mice. Acyl-CoA: diacylglycerol acyltransferase (DGAT) is responsible for the final esterification step of diacylglycerol to triacylglycerol,[13] and acyl-CoA:glycerol-3-phosphate acyltransferase (GPAT) is responsible for the first esterification step of glycerol-3-phosphate to monoacylglycerol.[16] Both are involved in TG synthesis but were not increased in sucrose-supplemented mice (Fig. 5). Carbohydrate response element-binding protein (ChREBP) binds to and activates the transcription of several lipogenic enzyme genes such as those for liver-type pyruvate kinase (LPK), a regulatory enzyme in the hepatic glycolysis pathway, ACC1, and FAS, leading to fatty liver.[17] LPK mRNA was increased in sucrose-supplemented mice (Fig. 5). Activation of peroxisome proliferator-activated receptor (PPAR) $\gamma$ causes fatty liver. Hepatic PPAR$\gamma$ expression is increased in several animal models of diabetes and obesity.[18,19] Adenovirus delivery of PPAR$\gamma$ in hepatocytes leads to fatty liver,[20] and PPAR$\gamma$ RNA interference is reported to decrease hepatic TG levels.[21] Therefore, expression levels of PPAR$\gamma$ mRNA and that of its target, fatty acid translocase (CD36), were measured. PPAR$\gamma$ consists of 2 forms, PPAR$\gamma$1 and PPAR$\gamma$2, and both forms are expressed in hepatocytes. However, mRNAs for both isoforms were not altered in sucrose-supplemented mice (Fig. 6). Sucrose supplementation may inhibit PPAR$\alpha$, which increases fatty acid $\beta$ oxidation in the liver.[22] However, mRNA levels of PPAR$\alpha$ and its target genes, including acyl-CoA oxidase (ACO, a marker of peroxisomal $\beta$-oxidation), medium-chain acyl-CoA dehydrogenase (MCAD, a marker of mitochondrial $\beta$-oxidation), and carnitine palmitoyltransferase 1 (CPT1, a marker of fatty acid transport), were not altered in sucrose-supplemented mice (Fig. 6). These data suggested that sucrose supplementation activates the transcription factors SREBP-1c and ChREBP and promotes fatty acid synthesis.

***Effects of High-Safflower Oil on Fatty Liver.*** The mechanisms underlying the development of fatty liver in mice fed a high-safflower oil diet (relative to high-starch–fed mice) were elucidated by hepatic gene expression profiling. High-safflower oil–fed mice did not show altered expression of SREBP-1c, SREBP-1a, FAS, ACC1, DGATs, GPAT, ChREBP, or LPK mRNA but did show decreased SCD1 mRNA (Fig. 5). High-safflower oil increased PPAR$\gamma$1, PPAR$\gamma$2, and CD36 mRNAs, although these increases were not significant (Fig. 6). High-safflower oil slightly increased ACO, CPT1, and MCAD mRNAs, but only the increase in ACO mRNA was significant (Fig. 6).

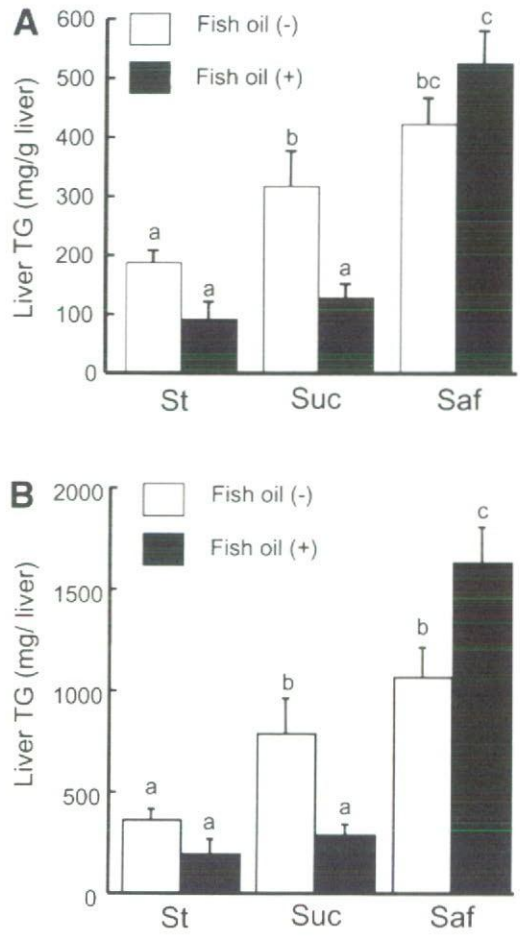


Fig. 2. Fish oil prevents sucrose-induced hepatic TG accumulation (Suc) but not high-safflower oil-induced TG accumulation (Saf). (A) Hepatic lipids were extracted, and TG concentrations were measured. (B) TG content in a whole liver of mouse. Values are mean ± SEM (n = 5-9). Means without a common letter differ ($P < 0.05$). Two-way ANOVA $P$ values are significant in effects of diet and interaction. St, high-starch diet.

***Effects of Fish Oil Supplementation on Control, High-Starch Diet-Fed Mice.*** Fish oil decreased SCD-1 and LPK mRNAs and increased ACO mRNA significantly (Figs. 5 and 6). Fish oil–mediated suppression of SREBP-1c and ChREBP activity may lead to a decrease in liver TG content in high-starch–fed mice.

***Effects of Fish Oil Supplementation on Sucrose-Supplemented Mice.*** Fish oil significantly decreased FAS, SCD1, and ACC1 mRNAs (Fig. 5). The transcription factor liver X receptor (LXR)$\alpha$ binds to the SREBP-1c promoter and increases its expression[23]; however, fish oil did not significantly decrease the LXR$\alpha$ mRNA level. The coactivator peroxisome proliferator-activated receptor $\gamma$ coactivator (PGC)-1 $\beta$ binds to SREBP-1c and activates its transcriptional activity[24]; however, the PGC-1$\beta$ mRNA levels were not altered. These data indicated that repression of sucrose-induced SREBP-1c activation may lead to a decrease in liver TG content.

***Effects of Fish Oil Supplementation on High-Safflower Oil–Fed Mice.*** Fish oil increased SREBP-1a, SCD1, and GPAT mRNAs (Fig. 5). However, these increases were not observed in experiment II. The reason for this discrepancy is unknown, but it suggests that increased expression of these genes is not important for the fish oil–induced liver TG increase. Surprisingly, fish oil markedly increased the expression of PPAR$\gamma$1, PPAR$\gamma$2, and CD36 mRNAs (Fig. 6). PPAR$\gamma$ expression is suppressed by the transcription factor hairy enhancer of split (HES-1), and HES-1 expression is increased by the cyclic adenosine monophosphate–responsive transcription factor-binding protein (CREB). This pathway is involved in the inhibition of hepatic TG synthesis observed in fasting.[21] However, HES-1 and CREB mRNAs were not altered. Fish oil did not alter the PPAR$\alpha$ mRNA level, but it did increase ACO, CPT1, and MCAD mRNAs, suggesting that PPAR$\alpha$ activation may not be sufficient to decrease the TG accumulation in these mice. Therefore, the exacerbation of fatty liver may be attributable to increased PPAR$\gamma$ expression.

***High-Butter-Fed Mice Show Increased Liver TG Concentration Compared with High-Safflower Oil–Fed Mice, But Fish Oil Does Not Exacerbate High-Butter–Induced Fatty Liver.*** To examine the mechanism(s) underlying the exacerbation of fatty liver by fish oil in mice fed a high-safflower oil, we fed mice butter, saturated fatty acid–rich oil, with or without fish oil supplementation, in experiment II. As negative and positive controls, mice were fed a high-starch diet and a high-safflower oil diet, respectively. Energy intake was similar between high-safflower oil–fed and high-butter–fed mice and between fish oil–supplemented and non-supplemented mice (data not shown). Because the 2 HF diets are hypercaloric and contain the same amount of other nutrients, we limited statistical comparisons to the effects of the 2 HF diets rather than comparing them with the effects of the high-starch diet (Tables 4-6). After 11 weeks, high-butter–fed mice showed increases in body weight and liver and epididymal WAT weights (relative to high-safflower oil-fed mice), but these increases were not significant. The liver TG concentration in high-butter–fed mice was twice that in high-safflower oil–fed mice (Table 4). As observed in experiment I, fish oil further increased the liver TG content in high-safflower oil–fed mice; surprisingly, this exacerbation was not observed in high-butter–fed mice (Table 4).

***Postprandial TG Concentrations Are Increased in Mice Fed Safflower Oil or Butter, and Fish Oil Causes Insulin Resistance in Mice Fed High-Safflower Oil.*** Increased plasma concentrations of glucose and NEFA may promote hepatic steatosis.[25] In experiment II, we

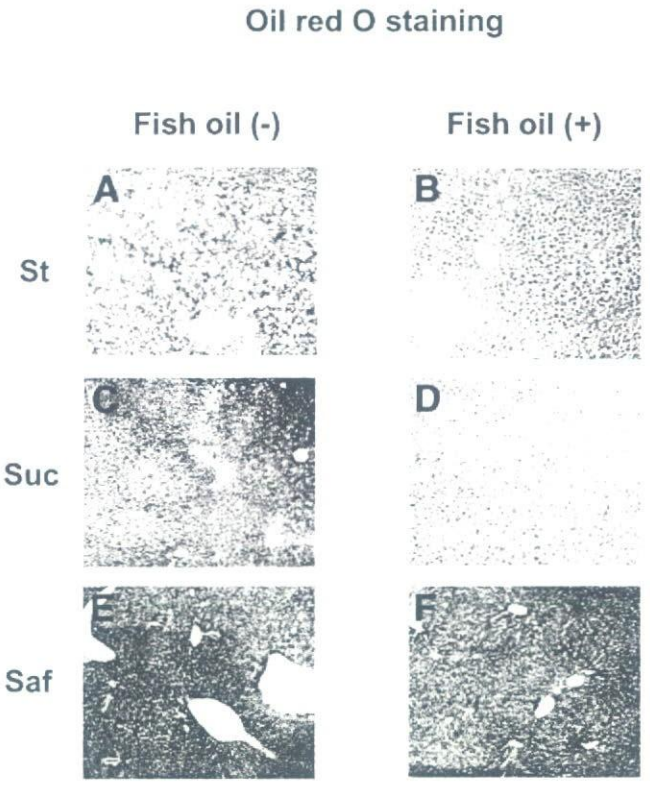


Fig. 3. Oil red O staining of liver sections from mice fed high-starch (St) (A), high-starch plus fish oil (B), sucrose (Suc) (C), sucrose plus fish oil (D), high-safflower oil (Saf) (E), and high-safflower oil plus fish oil (F) for 11 weeks. Fish oil markedly decreased hepatic TG accumulation in sucrose-supplemented mice (D) but not in high-safflower oil–fed mice (F).

measured serum glucose, NEFA, TG, and insulin concentrations at 2 points, after 24 hours of fasting (fasting) and 3 hours after refeeding (postprandial). Fish oil increased fasting glucose and insulin concentrations in high-safflower oil–fed mice but not in high-butter–fed mice (Table 5). We estimated insulin sensitivity by the Quantitative Insulin Sensitivity Check Index[26] (QUICKI; see Table 5 legend for formula). Fish oil decreased insulin sensitivity in high-safflower oil–fed mice but not in high-butter–fed mice, suggesting that the interaction of fish oil and safflower oil may lead to insulin resistance. Postprandial glucose and insulin concentrations were not altered. Fish oil decreased the postprandial NEFA concentration in high-butter–fed mice but not in high-safflower oil–fed mice, suggesting that relatively increased postprandial NEFA may contribute to fish oil–induced liver TG accumulation in high-safflower oil–fed mice. The postprandial TG concentration was increased both in high-safflower oil–fed and butter-fed mice (relative to high-starch–fed mice), and fish oil decreased the postprandial TG concentration by 28% and 18%, respectively, but these decreases were not significant.

***Fish Oil Increases PPARγ Expression in Safflower Oil–Fed Mice But Not in Butter-Fed Mice.*** Hepatic gene expression profiles are shown in Table 6. Fish oil markedly decreased SREBP-1c and target gene mRNAs in high-butter–fed mice but not in high-safflower oil–fed mice. Fish oil increased expression of PPARγ1 and CD36 mRNAs in high-safflower oil–fed mice, but decreased expression in high-butter–fed mice, although these decreases were not significant. However, fish oil did not decrease liver TG content in high-butter–fed mice, suggesting that increased postprandial TG, which supplies a large amount of fat to the liver, may overwhelm decreased fat synthesis in the liver.

## Discussion

In this study, we found that the effects of fish oil on fatty liver differ according to the cause of fatty liver. In the dietary models of fatty liver, fish oil supplementation showed different effects on hepatic TG accumulation. Fish oil completely prevented sucrose-induced fatty liver, whereas it exacerbated high-safflower oil–induced fatty liver. Fish oil did not affect high-butter–induced fatty liver. Sucrose supplementation increased SREBP-1c expression and induced lipogenesis, and this process was effectively inhibited by fish oil supplementation. Fish oil increased the expression of hepatic PPARγ mRNA in high-safflower oil–fed mice, which may worsen fatty liver,

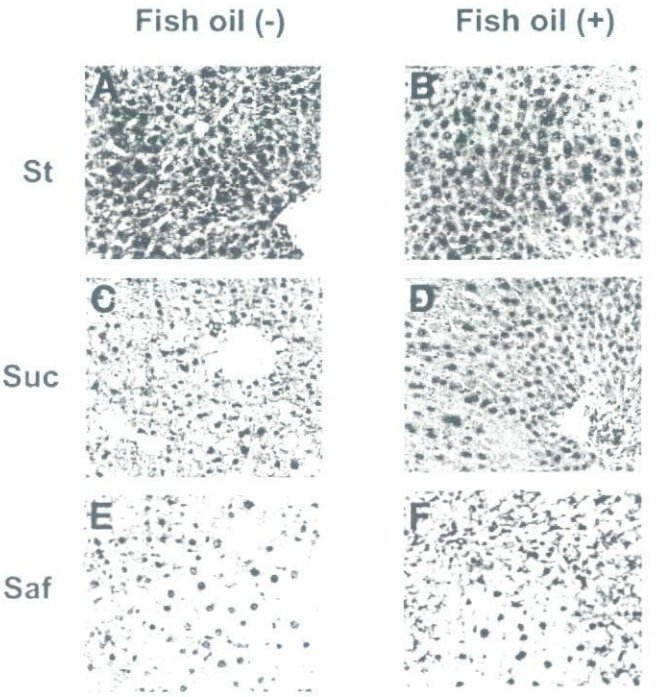


Fig. 4. Comparative liver morphology as revealed in sections stained with hematoxylin-eosin. Microvesicular fatty change in hepatocytes is observed in sucrose-supplemented (Suc) (C) and high-safflower oil-fed (Saf) mice (E). Note the absence of microvesicular fatty change in sucrose-supplemented plus fish oil-supplemented mice (D).

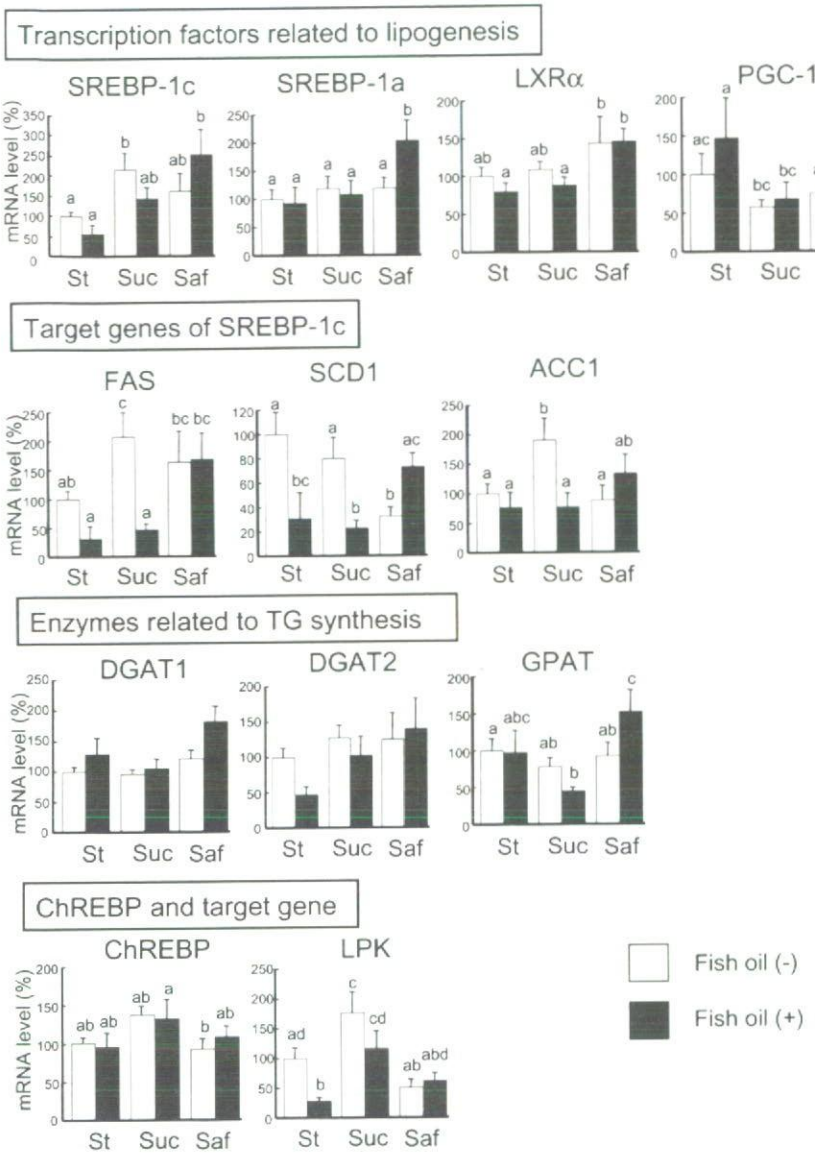


Fig. 5. Hepatic gene expression of transcription factors related to lipogenesis, target genes of SREBP-1c, enzymes related to TG synthesis, and ChREBP and LPK in mice fed high-starch (St), sucrose supplementation (Suc), and high-safflower oil (Saf) with or without fish oil for 11 weeks in experiment I. Quantitative PCR analysis was performed with the specific primers listed in Table 2. Values are mean ± SEM ($n$ = 5-9). Means without a common letter differ ($P < 0.05$). The percentage in mRNA levels relative to those of high-starch fed mice without fish oil are shown. Two-way ANOVA $P$ values with respect to diet effect are significant for SREBP-1c, SREBP-1a, LXRα, FAS, DGAT1, GPAT, ChREBP, and LPK; with respect to fish oil effects are significant for FAS, SCD1, and DGAT1; those with respect to interaction are significant for SCD1, ACC1, and GPAT.

whereas this increase was not observed in sucrose-supplemented mice or high-butter oil–fed mice.

The role of SREBP-1c in sucrose/fructose-induced fatty liver has been examined extensively. In mice with on a pure 129 SV background, fructose supplementation induces fatty liver.[27] Fructose induces the hepatic expression of SCD1 and other lipogenic proteins in SREBP-1c-knockout mice, but not in SCD1-knockout mice,[27] indicating that SCD1 expression is important for the development of fructose-induced fatty liver. However, in ddY mice, sucrose supplementation increased SREBP-1c mRNA and that of its target genes FAS and ACC1 but did not affect SCD1 mRNA expression (Fig. 5), suggesting that the induction of SCD1 is not always necessary for the development of fatty liver. In Wistar rats, increases in hepatic FAS and malic enzyme mRNAs were observed in response to a high-sucrose diet, and fish oil suppressed these increases.[28] In ddY mice, fish oil decreased hepatic TG accumulation, along with a decrease in FAS and SCD1 mRNAs in response to sucrose supplementation. Therefore, fish oil may prevent sucrose-induced fatty liver by inhibiting the effects of lipogenic enzymes.

The mechanism of fatty liver in response to a HF diet has also been examined. In Fisher 344 rats, those fed a large amount of lard (45 en%) showed 3.7-fold greater hepatic TG concentration than those fed a large amount of fish oil (45 en%).[26] The postprandial TG concentration in lard-fed rats was 221 mg/dL, whereas that in fish oil-fed rats was 75 mg/dL, suggesting that the increased amount of absorbed fat may be responsible for TG accumulation in the liver.[26] In experiment II, we also observed increased postprandial TG concentration in high-butter–fed and high-safflower oil–fed mice (relative to high-starch–fed mice); however, fish oil slightly inhibited this

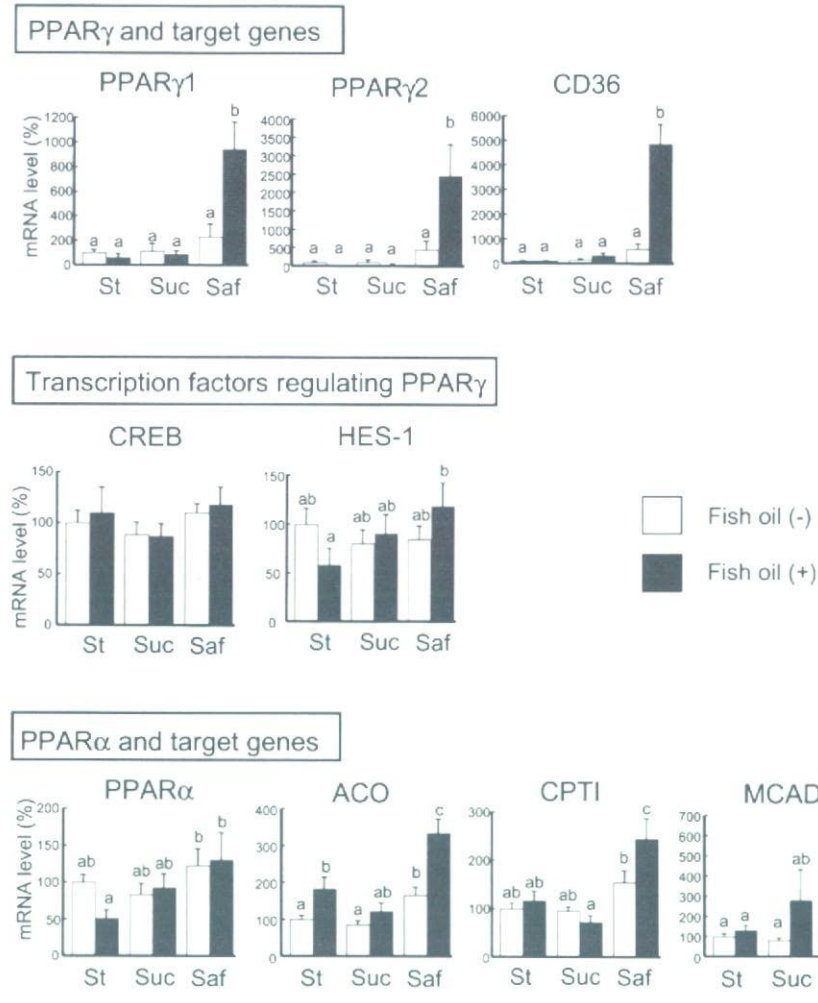


Fig. 6. Hepatic gene expression of PPARγ and PPARα and their target genes and of transcription factors regulating PPARγ in mice fed high-starch (St), sucrose supplementation (Suc), and high-safflower oil (Saf) with or without fish oil for 11 weeks in experiment I. Quantitative PCR analysis was performed with the specific primers listed in Table 2. Values are mean ± SEM ($n = 5$-9). Means without a common letter differ ($P < 0.05$). The percentage in mRNA levels relative to those of high-starch–fed mice without fish oil are shown. Two-way ANOVA $P$ values with respect to diet effect are significant for PPARγ1, PPARγ2, CD36, ACO, CPT1, and MCAD; those with respect to fish oil effects are significant for PPARγ1, CD36, ACO, and MCAD; those with respect to interaction are significant for PPARγ1, PPARγ2, CD36, and ACO.

increase. The difference in the decrease in postprandial TG by fish oil in these 2 studies may be attributable to a difference in the dose of fish oil (45 en% versus 10 en%). However, the fish oil–induced liver TG increase in high-safflower oil–fed mice was not explained by alterations in postprandial TG concentration.

With respect to hepatic gene expression profiles, HF diet (36-82 en%)-fed C57BL/6J mice show fatty liver without increases in SREBP-1c or target gene mRNAs[8-10] but increased PPARγ and target gene mRNAs.[9,10] However, the dietary fatty acid compositions were not described in these studies. In the current study, fish oil further increased PPARγ and target gene mRNAs, when given to mice fed high-safflower oil diet but not to mice fed high-butter diet. This may be a major reason why fish oil exacerbates high-safflower oil–induced fatty liver, despite increased PPARα activation and decreased postprandial serum TG concentration, which may favor a decrease in liver TG. Insulin increases the expression of PPARγ2 in human adipocytes and in mouse hepatocytes.[29,30] An increased fasting blood insulin level may increase PPARγ expression. We speculate that unknown interactions between safflower oil and fish oil may lead to insulin resistance (lower QUICKI in Table 5), and fasting hyperinsulinemia attributable to insulin resistance may up-regulate PPARγ mRNA, which leads to the exacerbation of fatty liver. It is unlikely that fatty liver causes hyperinsulinemia because high-butter–fed mice did not show this condition. Sustained fatty acid synthesis in response to fish oil in high-safflower oil–fed mice could also be the consequence of fasting hyperinsulinemia; insulin is known to enhance both the transcription and activation of SREBP-1c.[31]

The increase in fatty liver in response to fish oil is probably attributable to the additive effects of several factors: increased PPARγ, high serum NEFA, and insulin resistance, as well as an absence of inhibition of fatty acid synthesis. Thus, the balance is toward fat accumulation.

In humans, overconsumption of sucrose/fructose or fat are 2 major causes of fatty liver. With the use of stable isotopes, it has been shown that in healthy men, a high-fructose diet increased the fractional de novo lipogenesis by 6-fold and that supplementation with fish oil (7.2

**Table 4. Body and Tissue Weights and Liver TG of Mice After 11 Weeks on Study Diets in Experiment II**

| | | | | | Two-Way ANOVA *P* Value | | |
|---|---|---|---|---|---|---|---|
| | | St | Saf | Butter | Fat | Fish Oil | Fat × Fish Oil |
| | Fish oil | | | | | | |
| n | − | 8 | 8 | 8 | | | |
| | + | 7 | 8 | 8 | | | |
| Weight (g) | | | | | | | |
| BW at start | − | 34.3 ± 0.5 | 34.3 ± 0.5 | 34.3 ± 0.3 | | | |
| | + | 34.6 ± 0.4 | 34.4 ± 0.4 | 34.2 ± 0.4 | 0.859 | 0.976 | 0.882 |
| Final BW | − | 49.3 ± 2.0 | 55.9 ± 1.5 | 60.3 ± 1.0 | | | |
| | + | 49.7 ± 1.4 | 58.2 ± 1.5 | 57.0 ± 2.3 | 0.341 | 0.757 | 0.097 |
| Liver | − | 1.73 ± 0.07 | 2.19 ± 0.11 | 2.63 ± 0.17 | | | |
| | + | 1.82 ± 0.09 | 2.74 ± 0.21 | 2.46 ± 0.28 | 0.711 | 0.354 | 0.082 |
| Epididymal WAT | − | 2.01 ± 0.22 | 2.48 ± 0.29 | 3.05 ± 0.28 | | | |
| | + | 1.69 ± 0.20 | 2.31 ± 0.25 | 2.48 ± 0.12 | 0.135 | 0.142 | 0.415 |
| Liver TG (mg/g liver) | − | 124 ± 10 | 240 ± 37$^{a}$ | 473 ± 59$^{b}$ | | | |
| | + | 103 ± 19 | 357 ± 61$^{ab}$ | 468 ± 109$^{b}$ | 0.023 | 0.438 | 0.400 |
| Liver TG (mg/liver) | − | 218 ± 23 | 547 ± 81$^{a}$ | 1307 ± 180$^{b}$ | | | |
| | + | 194 ± 43 | 1037 ± 108$^{b}$ | 1304 ± 207$^{b}$ | 0.002 | 0.122 | 0.119 |

Abbreviations: St, high-starch diet; Saf, high-safflower oil diet; BW, body weight; WAT, white adipose tissue. Values are mean ± SEM. Means without a common letter differ ($P < 0.05$).

g/day) partially prevents this increase.[32] It is likely that most humans are responders to sucrose/fructose overconsumption and that fish oil supplementation inhibits sucrose-induced fatty liver. With respect to HF diet–induced fatty liver, patients with fatty liver have been shown to consume significantly more saturated fat per day than control subjects matched for body mass index.[33] The amount of hepatic fat appears to be related to the amount

**Table 5. Serum Analysis of Mice After 11 Weeks on Study Diets in Experiment II**

| | | | | | Two-Way ANOVA *P* Value | | |
|---|---|---|---|---|---|---|---|
| | | St | Saf | Butter | Fat | Fish Oil | Fat × Fish Oil |
| | Fish oil | | | | | | |
| n | − | 8 | 8 | 8 | | | |
| | + | 7 | 8 | 8 | | | |
| Serum analysis | | | | | | | |
| Glucose (mg/dL) | | | | | | | |
| 0h | − | 92 ± 5 | 112 ± 7$^{a}$ | 106 ± 6$^{a}$ | | | |
| | + | 82 ± 6 | 142 ± 9$^{b}$ | 95 ± 8$^{a}$ | 0.002 | 0.211 | 0.012 |
| 3h | − | 189 ± 11 | 147 ± 9 | 151 ± 12 | | | |
| | + | 195 ± 15 | 138 ± 8 | 155 ± 11 | 0.336 | 0.827 | 0.537 |
| NEFA (mEq/L) | | | | | | | |
| 0h | − | 1.07 ± 0.13 | 1.27 ± 0.11$^{ab}$ | 1.41 ± 0.15$^{bc}$ | | | |
| | + | 1.06 ± 0.13 | 1.02 ± 0.09$^{a}$ | 1.13 ± 0.08$^{ab}$ | 0.257 | 0.023 | 0.916 |
| 3h | − | 0.85 ± 0.09 | 1.58 ± 0.15$^{a}$ | 1.97 ± 0.18$^{a}$ | | | |
| | + | 0.91 ± 0.11 | 1.57 ± 0.09$^{a}$ | 1.11 ± 0.12$^{b}$ | 0.786 | 0.004 | 0.006 |
| TG (mg/dL) | | | | | | | |
| 0h | − | 140 ± 17 | 189 ± 25 | 189 ± 23 | | | |
| | + | 197 ± 22 | 153 ± 19 | 167 ± 21 | 0.736 | 0.193 | 0.762 |
| 3h | − | 184 ± 31 | 380 ± 63$^{ab}$ | 519 ± 94$^{bc}$ | | | |
| | + | 229 ± 30 | 274 ± 42$^{a}$ | 426 ± 49$^{ab}$ | 0.034 | 0.138 | 0.926 |
| Insulin (ng/mL) | | | | | | | |
| 0h | − | 0.28 ± 0.13 | 0.34 ± 0.08$^{a}$ | 0.38 ± 0.06$^{a}$ | | | |
| | + | 0.35 ± 0.15 | 1.28 ± 0.35$^{b}$ | 0.32 ± 0.08$^{a}$ | 0.020 | 0.027 | 0.013 |
| 3h | − | 4.33 ± 0.76 | 5.54 ± 1.39 | 5.75 ± 0.75 | | | |
| | + | 7.74 ± 1.18 | 6.86 ± 1.60 | 6.78 ± 1.53 | 0.961 | 0.396 | 0.913 |
| QUICKI | − | 0.385 ± 0.029 | 0.342 ± 0.013$^{a}$ | 0.333 ± 0.009$^{ab}$ | | | |
| | + | 0.374 ± 0.024 | 0.290 ± 0.015$^{b}$ | 0.365 ± 0.021$^{a}$ | 0.041 | 0.527 | 0.011 |

Abbreviations: St, high-starch diet; Saf, high-safflower oil diet; 0h, serum obtained from 24-hour-fasted mice; 3h, serum obtained from animals 3 hours after food was presented; QUICKI, Quantitative Insulin Sensitivity Check Index, which is calculated by the following formula: 1/[loginsulin+logglucose], where insulin concentration is measured in microunit per milliliter and glucose concentration in milligram per deciliter. Values are mean ± SEM. Means without a common letter differ ($P < 0.05$).

**Table 6. Hepatic Gene Expression Profile Related to TG Synthesis of Mice After 11 Weeks on Study Diets in Experiment II**

| | | | | | Two-Way ANOVA *P* Value | | |
|---|---|---|---|---|---|---|---|
| | | St | Saf | Butter | Fat | Fish Oil | Fat × Fish Oil |
| | Fish oil | | | | | | |
| n | − | 8 | 8 | 8 | | | |
| | + | 7 | 8 | 8 | | | |
| Transcription factors related to lipogenesis | | | | | | | |
| SREBP-1c | − | 100 ± 18 | 114 ± 24$^{ab}$ | 151 ± 25$^{b}$ | | | |
| | + | 51 ± 22 | 123 ± 31$^{b}$ | 52 ± 6$^{a}$ | 0.484 | 0.063 | 0.029 |
| SREBP-1a | − | 100 ± 8 | 101 ± 7 | 104 ± 12 | | | |
| | + | 96 ± 21 | 109 ± 15 | 72 ± 7 | 0.127 | 0.274 | 0.078 |
| LXR$\alpha$ | − | 100 ± 10 | 103 ± 8 | 85 ± 10 | | | |
| | + | 102 ± 18 | 112 ± 13 | 90 ± 8 | 0.049 | 0.513 | 0.818 |
| PGC-1$\beta$ | − | 100 ± 17 | 92 ± 8 | 111 ± 29 | | | |
| | + | 147 ± 30 | 118 ± 28 | 65 ± 13 | 0.435 | 0.631 | 0.106 |
| Target tenes or SREBP-1c | | | | | | | |
| FAS | − | 100 ± 8 | 84 ± 24$^{a}$ | 136 ± 38$^{a}$ | | | |
| | + | 29 ± 4 | 74 ± 13$^{ab}$ | 14 ± 2$^{b}$ | 0.867 | 0.009 | 0.024 |
| SCD1 | − | 100 ± 11 | 18 ± 6$^{ac}$ | 54 ± 11$^{b}$ | | | |
| | + | 34 ± 17 | 24 ± 6$^{a}$ | 1 ± 1$^{c}$ | 0.389 | 0.003 | <0.001 |
| ACC1 | − | 100 ± 4 | 69 ± 11$^{a}$ | 88 ± 14$^{a}$ | | | |
| | + | 77 ± 29 | 67 ± 6$^{a}$ | 29 ± 4$^{b}$ | 0.316 | 0.004 | 0.007 |
| Enzymes related to TG synthesis | | | | | | | |
| DGAT1 | − | 100 ± 9 | 87 ± 7 | 76 ± 7 | | | |
| | + | 102 ± 13 | 79 ± 6 | 69 ± 6 | 0.136 | 0.256 | 0.958 |
| DGAT2 | − | 100 ± 9 | 108 ± 12 | 104 ± 16 | | | |
| | + | 119 ± 19 | 92 ± 13 | 90 ± 9 | 0.821 | 0.260 | 0.932 |
| GPAT | − | 100 ± 23 | 87 ± 9$^{ab}$ | 141 ± 14$^{cd}$ | | | |
| | + | 110 ± 38 | 106 ± 19$^{bd}$ | 51 ± 5$^{a}$ | 0.950 | 0.039 | 0.002 |
| ChREBP and target gene | | | | | | | |
| ChREBP | − | 100 ± 18 | 103 ± 12 | 102 ± 20 | | | |
| | + | 97 ± 19 | 106 ± 16 | 79 ± 10 | 0.361 | 0.511 | 0.388 |
| LPK | − | 100 ± 17 | 34 ± 6$^{a}$ | 61 ± 11$^{b}$ | | | |
| | + | 37 ± 8 | 39 ± 4$^{a}$ | 29 ± 8$^{a}$ | 0.245 | 0.087 | 0.022 |
| PPAR$\gamma$ and target genes | | | | | | | |
| PPAR$\gamma$1 | − | 100 ± 23 | 405 ± 110$^{a}$ | 315 ± 149$^{a}$ | | | |
| | + | 113 ± 33 | 1043 ± 287$^{b}$ | 143 ± 60$^{a}$ | 0.008 | 0.190 | 0.027 |
| PPAR$\gamma$2 | − | 100 ± 15 | 587 ± 244$^{ab}$ | 952 ± 396$^{ab}$ | | | |
| | + | 32 ± 5 | 1030 ± 220$^{b}$ | 240 ± 53$^{a}$ | 0.420 | 0.608 | 0.034 |
| CD36 | − | 100 ± 8 | 185 ± 57$^{a}$ | 161 ± 33$^{a}$ | | | |
| | + | 97 ± 10 | 435 ± 92$^{b}$ | 123 ± 37$^{a}$ | 0.009 | 0.089 | 0.023 |
| Transcription factors regulating PPAR$\gamma$ | | | | | | | |
| CREB | − | 100 ± 14 | 110 ± 11 | 106 ± 11 | | | |
| | + | 118 ± 24 | 123 ± 13 | 93 ± 14 | 0.177 | 0.980 | 0.305 |
| HES-1 | − | 100 ± 18 | 103 ± 12 | 102 ± 20 | | | |
| | + | 97 ± 19 | 106 ± 16 | 79 ± 10 | 0.361 | 0.512 | 0.388 |
| PPAR$\alpha$ and their target genes | | | | | | | |
| PPAR$\alpha$ | − | 100 ± 10 | 102 ± 12 | 87 ± 11 | | | |
| | + | 114 ± 14 | 97 ± 13 | 76 ± 6 | 0.109 | 0.458 | 0.787 |
| ACO | - | 100 ± 8 | 114 ± 18$^{ab}$ | 99 ± 17$^{a}$ | | | |
| | + | 159 ± 27 | 159 ± 16$^{b}$ | 97 ± 14$^{a}$ | 0.027 | 0.214 | 0.158 |
| CPTI | - | 100 ± 11 | 107 ± 12$^{ab}$ | 83 ± 11$^{ac}$ | | | |
| | + | 121 ± 19 | 119 ± 15$^{b}$ | 70 ± 5$^{c}$ | 0.004 | 0.984 | 0.306 |
| MCAD | - | 100 ± 9 | 132 ± 14$^{ad}$ | 88 ± 11$^{bc}$ | | | |
| | + | 155 ± 24 | 169 ± 14$^{a}$ | 121 ± 15$^{cd}$ | 0.002 | 0.014 | 0.873 |

Abbreviations: St, high-starch diet; Saf, high-safflower oil diet; BW, body weight; WAT, white adipose tissue.

Values are mean ± SEM. Means without a common letter differ ($P < 0.05$). The percentage in mRNA levels relative to those of high-starch-fed mice without fish oil are shown.

of fat in the diet rather than to endogenous fat deposits in obese women,[34] suggesting that increased postprandial TG may favor fatty liver formation. In the current study, saturated fat–rich butter favored fatty liver formation more than did safflower oil, with greater postprandial TG concentration (Table 5).

The 10 en% fish oil (2.9 en% n-3 fatty acid) used in this study is comparable to levels consumed by humans. It is

likely that fish oil supplementation is most effective in preventing fatty liver in those overfeeding sucrose, but not in those in overfeeding fat. To prevent fatty liver in a HF diet, it may be effective to inhibit intestinal absorption of dietary fat.

## References


1. Clark JM, Brancati FL, Diehl AM. Nonalcoholic fatty liver disease. Gastroenterology 2002;122:1649-1657.
2. Bacon BR, Farahvash MJ, Janney CG, Neuschwander-Tetri BA. Nonalcoholic steatohepatitis: an expanded clinical entity. Gastroenterology 1994;107:1103-1109.
3. Donnelly KL, Smith CI, Schwarzenberg SJ, Jessurun J, Boldt MD, Parks EJ. Sources of fatty acids stored in liver and secreted via lipoproteins in patients with nonalcoholic fatty liver disease. J Clin Invest 2005;115:1343-1351.
4. Capanni M, Calella F, Biagini MR, Genise S, Raimondi L, Bedogni G, et al. Prolonged n-3 polyunsaturated fatty acid supplementation ameliorates hepatic steatosis in patients with non-alcoholic fatty liver disease: a pilot study. Aliment Pharmacol Ther 2006;23:1143-1151.
5. Kim HJ, Takahashi M, Ezaki O. Fish oil feeding decreases mature sterol regulatory element-binding protein 1 (SREBP-1) by down-regulation of SREBP-1c mRNA in mouse liver. A possible mechanism for down-regulation of lipogenic enzyme mRNAs. J Biol Chem 1999;274:25892-25898.
6. Nakatani T, Kim HJ, Kaburagi Y, Yasuda K, Ezaki O. A low fish oil inhibits SREBP-1 proteolytic cascade, while a high-fish-oil feeding decreases SREBP-1 mRNA in mice liver: relationship to anti-obesity. J Lipid Res 2003;44:369-379.
7. Surwit RS, Kuhn CM, Cochrane C, McCubbin JA, Feinglos MN. Diet-induced type II diabetes in C57BL/6J mice. Diabetes 1988;37:1163-1167.
8. Gregoire FM, Zhang Q, Smith SJ, Tong C, Ross D, Lopez H, et al. Diet-induced obesity and hepatic gene expression alterations in C57BL/6J and ICAM-1-deficient mice. Am J Physiol Endocrinol Metab 2002;282: E703-E713.
9. Kim S, Sohn I, Ahn JI, Lee KH, Lee YS, Lee YS. Hepatic gene expression profiles in a long-term high-fat diet-induced obesity mouse model. Gene 2004;340:99-109.
10. Inoue M, Ohtake T, Motomura W, Takahashi N, Hosoki Y, Miyoshi S, et al. Increased expression of PPARγ in high fat diet-induced liver steatosis in mice. Biochem Biophys Res Commun 2005;336:215-222.
11. Nagata R, Nishio Y, Sekine O, Nagai Y, Maeno Y, Ugi S, et al. Single nucleotide polymorphism (-468 G to A) at the promoter region of SREBP-1c associates with genetic defect of fructose-induced hepatic lipogenesis. J Biol Chem 2004;279:29031-29042.
12. Takeda M, Imaizumi M, Sawano S, Manabe Y, Fushiki T. Long-term optional ingestion of corn oil induces excessive caloric intake and obesity in mice. Nutrition 2001;17:117-120.
13. Yamazaki T, Sasaki E, Kakinuma C, Yano T, Miura S, Ezaki O. Increased very low density lipoprotein secretion and gonadal fat mass in mice overexpressing liver DGAT1. J Biol Chem 2005;280:21506-21514.
14. Horton JD, Shimomura I. Sterol regulatory element-binding proteins: activators of cholesterol and fatty acid biosynthesis. Curr Opin Lipidol 1999;10:143-150.
15. Shimano H, Horton JD, Hammer RE, Shimomura I, Brown MS, Goldstein JL. Overproduction of cholesterol and fatty acids causes massive liver enlargement in transgenic mice expressing truncated SREBP-1a. J Clin Invest 1996;98:1575-1584.
16. Thuresson ER. Inhibition of glycerol-3-phosphate acyltransferase as a potential treatment for insulin resistance and type 2 diabetes. Curr Opin Invest Drugs 2004;5:411-418.
17. Uyeda K, Yamashita H, Kawaguchi T. Carbohydrate responsive element-binding protein (ChREBP): a key regulator of glucose metabolism and fat storage. Biochem Pharmacol 2002;63:2075-2080.
18. Gavrilova O, Haluzik M, Matsusue K, Cutson JJ, Johnson L, Dietz KR, et al. Liver peroxisome proliferator-activated receptor γ contributes to hepatic steatosis, triglyceride clearance, and regulation of body fat mass. J Biol Chem 2003;278:34268-34276.
19. Matsusue K, Haluzik M, Lambert G, Yim SH, Gavrilova O, Ward JM, et al. Liver- specific disruption of PPARγ in leptin-deficient mice improves fatty liver but aggravates diabetic phenotypes. J Clin Invest 2003;111:737-747.
20. Yu S, Matsusue K, Kashireddy P, Cao WQ, Yeldandi V, Yeldandi AV, et al. Adipocyte- specific gene expression and adipogenic steatosis in the mouse liver due to peroxisome proliferator-activated receptor γ1 (PPARγ1) overexpression. J Biol Chem 2003;278:498-505.
21. Herzig S, Hedrick S, Morantte I, Koo SH, Galimi F, Montminy M. CREB controls hepatic lipid metabolism through nuclear hormone receptor PPAR-γ. Nature 2003;426:190-193.
22. Reddy JK, Mannaerts GP. Peroxisomal lipid metabolism. Annu Rev Nutr 1994;14:343-370.
23. Repa JJ, Liang G, Ou J, Bashmakov Y, Lobaccaro JM, Shimomura I, et al. Regulation of mouse sterol regulatory element-binding protein-1c gene (SREBP-1c) by oxysterol receptors, LXRα and LXRβ. Genes Dev 2000; 14:2819-2830.
24. Lin J, Yang R, Tarr PT, Wu PH, Handschin C, Li S, et al. Hyperlipidemic effects of dietary saturated fats mediated through PGC-1β coactivation of SREBP. Cell 2005;120:261-273.
25. Chitturi S, Abeygunasekera S, Farrell GC, Holmes-Walker J, Hui JM, Fung C, et al. NASH and insulin resistance: Insulin hypersecretion and specific association with the insulin resistance syndrome. HEPATOLOGY 2002;35:373-379.
26. Levy JR, Clore JN, Stevens W. Dietary n-3 polyunsaturated fatty acids decrease hepatic triglycerides in Fischer 344 rats. HEPATOLOGY 2004;39: 608-616.
27. Miyazaki M, Dobrzyn A, Man WC, Chu K, Sampath H, Kim HJ, et al. Stearoyl-CoA desaturase 1 gene expression is necessary for fructose-mediated induction of lipogenic gene expression by sterol regulatory element-binding protein-1c-dependent and -independent mechanisms. J Biol Chem 2004;279:25164-25171.
28. Sebokova E, Klimes I, Gasperikova D, Bohov P, Langer P, Lavau M, et al. Regulation of gene expression for lipogenic enzymes in the liver and adipose tissue of hereditary hypertriglyceridemic, insulin-resistant rats: effect of dietary sucrose and marine fish oil. Biochim Biophys Acta 1996;1303:56-62.
29. Rieusset J, Andreelli F, Auboeuf D, Roques M, Vallier P, Riou JP, et al. Insulin acutely regulates the expression of the peroxisome proliferator-activated receptor-γ in human adipocytes. Diabetes 1999;48:699-705.
30. Edvardsson U, Ljungberg A, Oscarsson J. Insulin and oleic acid increase PPARγ2 expression in cultured mouse hepatocytes. Biochem Biophys Res Commun 2006;340:111-117.
31. Osborne TF. Sterol regulatory element-binding proteins (SREBPs): key regulators of nutritional homeostasis and insulin action. J Biol Chem 2000;275:32379-32382.
32. Faeh D, Minehira K, Schwarz JM, Periasamy R, Park S, Tappy L. Effect of fructose overfeeding and fish oil administration on hepatic de novo lipogenesis and insulin sensitivity in healthy men. Diabetes 2005;54:1907-1913.
33. Musso G, Gambino R, De Michieli F, Cassader M, Rizzetto M, Durazzo M, et al. Dietary habits and their relations to insulin resistance and postprandial lipemia in nonalcoholic steatohepatitis. HEPATOLOGY 2003;37: 909-916.
34. Tiikkainen M, Bergholm R, Vehkavaara S, Rissanen A, Hakkinen AM, Tamminen M, et al. Effects of identical weight loss on body composition and features of insulin resistance in obese women with high and low liver fat content. Diabetes 2003;52:701-707.

IMMUNOLOGY ORIGINAL ARTICLE

# Interleukin (IL)-4 promotes T helper type 2-biased natural killer T (NKT) cell expansion, which is regulated by NKT cell-derived interferon-γ and IL-4

Akira Iizuka,[1,4,5] Yoshinori Ikarashi,[1] Mitsuzi Yoshida,[1] Yuji Heike,[5] Kazuyoshi Takeda,[6] Gary Quinn,[3] Hiro Wakasugi,[2] Masanobu Kitagawa[4] and Yoichi Takaue[5]

[1]*Chemotherapy and* [2]*Pharmacology Divisions, and* [3]*Section for Studies on Metastasis, National Cancer Center Research Institute,* [4]*Department of Comprehensive Pathology, Aging and Developmental Sciences, Tokyo Medical and Dental University, Graduate School,* [5]*Hematopoietic Stem Cell Transplantation/Immunotherapy Unit, National Cancer Center Hospital, and* [6]*Department of Immunology, Juntendo University School of Medicine, Tokyo, Japan*

doi:10.1111/j.1365-2567.2007.02732.x
Received 31 January 2007; revised 20 August 2007; accepted 4 September 2007.
Correspondence: Dr Y. Ikarashi, Chemotherapy Division, National Cancer Center Research Institute, 5-1-1, Tsukiji, Chuo-ku, Tokyo 104-0045, Japan.
Email: yikarash@gan2.ncc.go.jp
Senior author: Dr Y. Ikarashi

## Summary

CD1d-restricted natural killer T (NKT) cells can rapidly produce T helper type 1 (Th1) and Th2 cytokines and also play regulatory or pathological roles in immune responses. NKT cells are able to expand when cultured with α-galactosylceramide (α-GalCer) and interleukin (IL)-2 in a CD1d-restricted manner. However, the expansion ratio of human NKT cells is variable from sample to sample. In this study, we sought to determine what factor or factors are responsible for efficient *in vitro* expansion of NKT cells from various inbred mouse strains. Although the proportion of NKT cells in the spleen was nearly identical in each mouse strain, the growth rates of NKT cells cultured *in vitro* with α-GalCer and IL-2 were highly variable. NKT cells from the B6C3F1 and BDF1 mouse strains expanded more than 20-fold after 4 days in culture. In contrast, NKT cells from the strain C3H/HeN did not proliferate at all. We found that cell expansion efficiency correlated with the level of IL-4 detectable in the supernatant after culture. Furthermore, we found that exogenous IL-4 augmented NKT cell proliferation early in the culture period, whereas interferon (IFN)-γ tended to inhibit NKT cell proliferation. Thus, the ratio of production of IL-4 and IFN-γ was important for NKT cell expansion but the absolute levels of these cytokines did not affect expansion. This finding suggests that effective expansion of NKT cells requires Th2-biased culture conditions.

**Keywords:** natural killer T cell; interleukin-4; interferon-γ; glycolipid

## Introduction

Mouse natural killer T (NKT) cells were initially identified as a T-cell subset that expresses NK cell receptors such as NK1·1, CD94 and Ly49.[1,2] The majority of NKT cells have the invariant T-cell receptor (TCR) α-chain rearrangement Vα14-Jα18 and recognize antigens presented by CD1d, a non-classical major histocompatibility complex (MHC) class I molecule.[3,4] NKT cells are continuously sensitized by endogenous antigens so that they display an effector-memory phenotype (such as $CD62L^{low}$ $CD44^{high}$)[5–7] and rapidly produce large amounts of T helper type 1 (Th1) and Th2 cytokines when stimulated with lipid antigens such as α-galactosylceramide (α-GalCer) in a CD1d-dependent manner.[2,8] NKT cells are regarded as immunoregulatory because of their cytokine profile. Moreover, NKT cells are thought to play an important role in response to infectious agents and in pathological responses such as allergies or autoimmune disease. NKT cells are cytotoxic to various tumour cell lines via Fas-ligand-, tumour necrosis factor-related apoptosis-inducing ligand (TRAIL)- and/or perforin-dependent pathways,[9–12] and play a role in tumour surveillance.[13] NKT cells activated by interleukin (IL)-12 or α-GalCer sequentially activate natural killer (NK) cells by producing interferon (IFN)-γ and induce antitumour immune responses. This in turn inhibits tumour metastasis and can suppress solid tumour growth. In some studies, it has been suggested that this ability helps to induce tumour antigen-specific CD8 T cells, thereby making an additional contribution to the immune response to cancer.[14]

In humans, counterparts of mouse NKT cells have also been found to be responsive to α-GalCer, which induces them to secrete IL-4 and IFN-γ. In addition, they have been shown to be cytotoxic to tumour cells via two different mechanisms, a CD1d-dependent and a CD1d-independent mechanism.[15] Human NKT cells have the

  

potential to induce antitumour responses *in vivo*. However, in patients with malignancies,[16,17] NKT cells are reduced in number and activity, and *in vivo* activation by α-GalCer leads to transient activation and long-term unresponsiveness of NKT cells.[18,19] For that reason, adaptive transfer of *in vitro* expanded and/or activated NKT cells is expected to induce effective antitumour responses.

To date, several combinations of cytokines with α-GalCer have been reported to expand NKT cells isolated from peripheral mononuclear cells. However, NKT cells present a diverse range of expansion ratios even among healthy individuals.[20,21] Although a previous study suggested that differences in NKT cell proliferation are associated with the age of the donor,[22] there is still much that remains to be determined concerning additional factors that influence NKT cell proliferation.

In this study, we used inbred mouse strains as an experimental system in which to reveal factors that affect variation in proliferation rates among individuals. Previously, we found that *in vitro* expanded NKT cells from C57BL/6 mice retained an effector-memory-like phenotype and retained the ability to produce cytokines.[23] In addition, we found that there was a marked difference in the NKT cell expansion ratio among various mouse strains and that the differences were closely related to the bias in production of Th1 or Th2 cytokines by NKT cells. Finally, we report that a relatively low rate of proliferation can be enhanced by the addition of IL-4, which creates Th2-biased culture conditions.

## Materials and methods

### *Mice*

Female C57BL/6N, BALB/cA, C3H/HeN, DBA/2N (C57BL/6 × DBA/2)$F_1$ (BDF1), (C57BL/6 × C3H/HeN)$F_1$ (B6C3F1), and SJL/J mice were purchased from Charles River Japan (Kanagawa, Japan). All mice, which were maintained in our animal facilities, were 8–11 weeks of age at the time of the experiment. All animal protocols for this study were reviewed and approved by the committee for ethics of animal experimentation at the National Cancer Center of Japan prior to the beginning of the study.

### *Monoclonal antibodies and reagents*

Anti-IL-4 (clone 11B11) and anti-IFN-γ (clone R4-6A2) monoclonal antigen-neutralizing antibodies (mAbs) were obtained from the supernatant of a hybridoma culture maintained in serum-free medium in a CELLine CL-1000 flask (BD Biosciences, San Jose, CA) and purified by Protein G Sepharose (GE Healthcare Amersham Biosciences AB, Uppsala, Sweden) affinity column chromatography. Anti-CD16/32 (clone 2·4G2) was obtained from a hybridoma supernatant. Fluorescein isothiocyanate (FITC)-conjugated anti-CD3 (clone 145-2C11), allophycocyanin (APC)-conjugated anti-IL-4 (11B11), anti-IFN-γ (XMG1·2), and a rat immunoglobulin G1 (IgG1) isotype control (clone R3-34) and Golgi Stop™ were obtained from BD Biosciences. α-Galactosylceramide (α-GalCer) was kindly provided by the Pharmaceutical Research Laboratory, KIRIN Brewery Co., Ltd (Gunma, Japan). The phycoerythrin (PE)-conjugated CD1d/α-GalCer tetramer was prepared using a baculovirus expression system as previously described.[24] Human recombinant IL-2 (rIL-2) was kindly provided by Takeda Chemical Industries Ltd (Osaka, Japan). Mouse rIL-4 was obtained from PeproTech EC Ltd (London, UK).

### *Flow cytometry*

NKT cells were detected by multicolour flow cytometry as previously described.[23] Briefly, cells were preincubated with anti-CD16/32 mAb to block non-specific FcRγ binding and then stained with FITC-conjugated anti-CD3 and PE-conjugated CD1d/α-GalCer tetramer. Dead cells were excluded by propidium iodide staining and electronic gating. For detection of intracellular cytokines, cells were stimulated for 3 hr with phorbol 12-myristate 13-acetate (PMA) (25 ng/ml) and ionomycin (1 μg/ml), with the last 1 hr of stimulation in the presence of Golgi block, in a 37°, 5% $CO_2$ incubator, and then washed and incubated with anti-CD16/32 mAb, followed by incubation with FITC-conjugated anti-CD3 and PE-conjugated CD1d/α-GalCer tetramer. Cells were then permeabilized using Cytofix/Cytoperm (BD Biosciences) and IL-4 or IFN-γ was detected using APC-conjugated mAbs. Cells were analysed by flow cytometry (FACSCalibur; BD Biosciences).

### *NKT cell proliferation assay*

Preparation of splenic mononuclear cells and *in vitro* expansion of NKT cells were performed as previously described.[23] Briefly, spleens of each mouse strain were macerated aseptically and pushed through a nylon mesh to obtain single-cell suspensions, and erythrocytes were lysed in ammonium chloride buffer. Mononuclear cells ($1 \times 10^6$ cells/ml) were cultured with α-GalCer (50 ng/ml) and rIL-2 (100 IU/ml) in RPMI-1640 culture medium (Sigma-Aldrich, St. Louis, MO) supplemented with 8% fetal calf serum (JRH Biosciences, Lenexa, KS), 2-mercaptoethanol ($5 \times 10^{-5}$ M) 100 U/ml penicillin and 100 μg/ml streptomycin for 4 days in a 37°, 5% $CO_2$ incubator. After 4 days in culture, the absolute number of living cells was counted using a microscope after staining of cells with 0·2% trypan blue, and the relative percentages of NKT cells were determined by flow cytometry.

### *Cytokine production*

The cell culture supernatant was collected after 24 hr or 4 days in culture and stored at −20°. The concentrations

of IL-4 and IFN-γ were determined by enzyme-linked immunosorbent assay (ELISA) (OptEIA ELISA set; BD Biosciences).

## Results

### α-GalCer-induced expansion of NKT cells from various mouse strains

Mouse NKT cells show a similar variation in expansion ratios to that observed for human NKT cells. We found that the expansion ratios were different for different mouse strains (Fig. 1). Before culture, spleen cell suspensions contained a small percentage (0·8–1·5%) and a small number (7–18 × $10^3$ cells/ml) of NKT cells in each mouse strain. As shown in Fig. 1, culture of spleen cells with α-GalCer and IL-2 induced expansion of NKT cells, except for C3H/HeN mice. After 4 days of culture, NKT cells constituted 6·4–40·7% of cells in the culture and had expanded 7–25-fold in BALB/c, C57BL/6, DBA/2, B6C3F1 and BDF1 mice. The CD1d-restricted TCR α-chain Vα14 dominantly associates with the high-affinity TCR β-chain Vβ8·2, or the lower affinity chain Vβ8·3, Vβ7 or Vβ2, and a genetic defect in Vβ8 is reportedly the cause of the low responsiveness of NKT cells. We next asked if the TCR-β status of NKT cells had an effect on expansion. However, we found no significant differences among the six strains that were tested, and selective proliferation did not occur (data not shown).

### NKT cell proliferation ratio correlates with amount of IL-4 in supernatant from a 4-day culture

Previously, a high concentration of IL-4 and IFN-γ in supernatant from a 4-day culture was observed.[23] Firstly, we measure amounts of IL-4 and IFN-γ in the culture supernatant.

An increase in the number of NKT cells was positively correlated with the production of IL-4 in the 4-day culture (Fig. 2a). However, high levels of IFN-γ were observed in all of the mouse strains, independent of an increase in either NKT cell number or IL-4 production. Almost all CD8 T cells acquired the ability to produce IFN-γ when activated indirectly via NKT cells by α-GalCer (data not shown), so it appears that, in C3H/HeN mice, NKT cells do not proliferate. Instead, it seems reasonable that a large amount of IFN-γ might be produced by the activated NK cells and CD8 T cells.[25,26]

A previous study reported cytokine secretion of NKT cells prior to their proliferation.[2,27] Thus, we harvested culture supernatants at 24 hr, before NKT cell expansion,[27] to determine the status of cytokine production at this early stage, which is the stage at which NKT cells initially respond to culture and initiate production of IL-4. This initial response positively correlated with NKT cell expansion to some degree, although the response was weaker than that observed for cells in culture for 4 days. It is notable that IL-4 production by C3H/HeN was more robust than that observed for C57BL/6, and IFN-γ

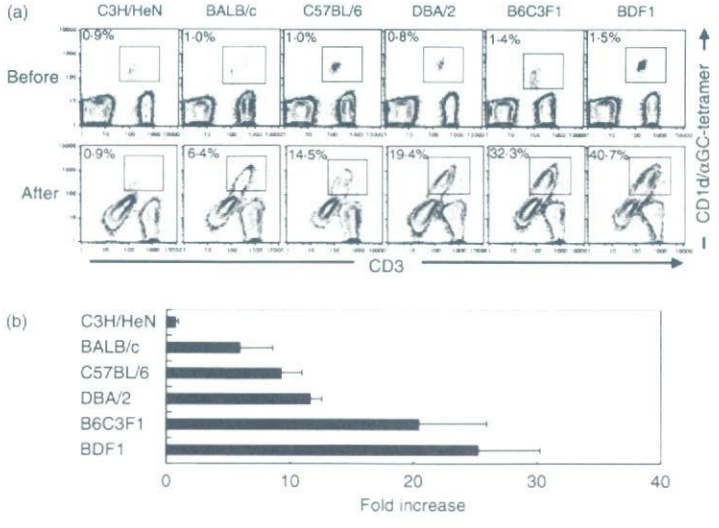


Figure 1. Expansion of natural killer T (NKT) cells *in vitro*. (a) Mouse spleen cells (1 × $10^6$ cells/ml) were cultured with 50 ng/ml α-galactosylceramide (α-GalCer) and 100 U/ml interleukin (IL)-2 for 4 days. Cells were stained with anti-CD3 monoclonal antibody (mAb) and CD1d/α-GalCer tetramer and analysed by flow cytometry. The percentage of NKT cells was determined for both fresh (upper row) and cultured (lower row) cells. Representative results from replicate experiments are shown. (b) The fold increase in NKT cells after culture was calculated based on living cell counts and the percentage of NKT cells in the total cell population. Data are shown as mean ± standard error of the mean ($n$ = 9 for C3H/HeN, BALB/c and C57BL/6; $n$ = 4 for DBA/2, B6C3F1 and BDF1).


 

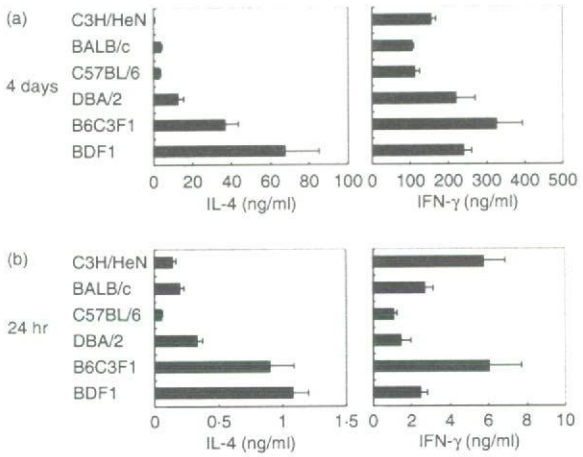


Figure 2. Production of interleukin (IL)-4 and interferon (IFN)-γ in expansion cell culture supernatants. Mouse spleen cells ($1 \times 10^6$ cells/ml) were cultured with 50 ng/ml α-galactosylceramide (α-GalCer) and 100 U/ml IL-2 for 4 days. Supernatants were collected after 24 hr (b) or 4 days (a). The levels of IFN-γ and IL-4 in the supernatants were determined by enzyme-linked immunosorbent assay (ELISA). Data are shown as mean ± standard error of the mean ($n = 9$ for C3H/HeN, BALB/c and C57BL/6; $n = 4$ for DBA/2, B6C3F1 and BDF1).

production of C3H/HeN mice was much higher than that of other strains (Fig. 2b). These observations lead us to speculate that IL-4 and IFN-γ produced by NKT cells work as promoting and suppressing factors, respectively, during NKT cell proliferation.

## NKT cell proliferation partially depends on IL-4 and is enhanced by Th2 cytokines

We next examined the influence of IL-4 on NKT cell proliferation *in vitro*. Proliferation of these cells was accelerated by addition of IL-4 at the start of the culture period, an effect that could be partially suppressed by neutralization of IL-4 (Fig. 3). In the C3H/HeN strain, where proliferation of NKT cells was not robust, a more significant induction of proliferation by IL-4 was observed (Fig. 4). In addition, neutralization of IFN-γ using antibodies did not significantly change the proportion of NKT cells in the total cell population. However, this did appear to up-regulate the total number of living cells and lead to a concomitant increase in the total number of NKT cells (Fig. 4b). Only NKT cells can produce IL-4 when cultured with α-GalCer and IL-2,[23] so IL-4 must act as an autocrine growth factor in the expansion of NKT cells in this context.

## The proportion of intracellular IFN-γ high positive NKT cells is reduced by addition of IL-4

Exogenous IL-4 promoted NKT cell expansion in C3H/HeN mice, as shown in Figs 3 and 4. We next examined

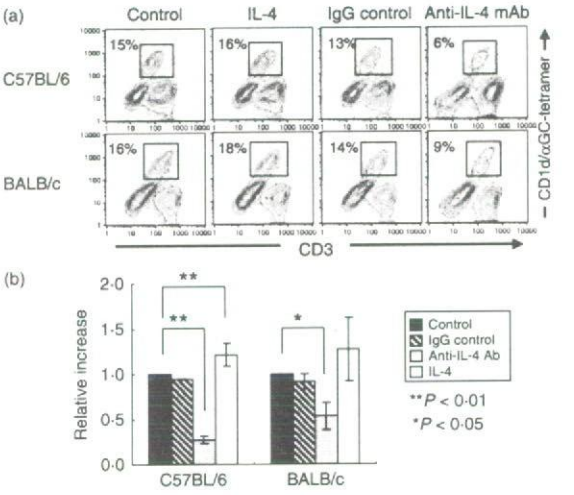


Figure 3. Expansion of natural killer T (NKT) cells in the presence or absence of interleukin (IL)-4. (a) Spleen cells ($1 \times 10^6$ cells/ml) were cultured with 50 ng/ml α-galactosylceramide (α-GalCer) and 100 U/ml IL-2 for 4 days with IL-4 (10 ng/ml) or anti-IL-4 monoclonal antibody (mAb) (1 mg/ml). The percentages of NKT cells are shown. Data are representative of replicate experiments. (b) The relative increase was based on absolute numbers of NKT cells and was compared with control expansion culture. Data are shown as mean ± standard deviation for five independent experiments. A paired two-tailed Student's *t*-test was used for statistical analysis (*$P < 0·05$; **$P < 0·01$).

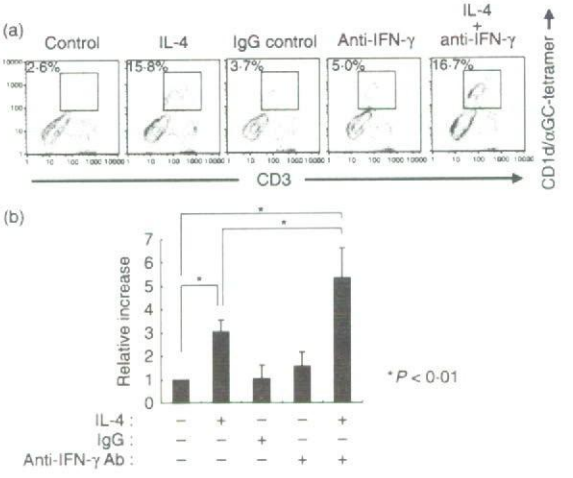


Figure 4. Expansion of natural killer T (NKT) cells from C3H/HeN strain mice in conditions that favour production of T helper type 2 (Th2)-biased cytokines. (a) Spleen cells ($1 \times 10^6$ cells/ml) were cultured with 50 ng/ml α-galactosylceramide (α-GalCer) and 100 U/ml interleukin (IL)-2 and with IL-4 (10 ng/ml) and/or anti-interferon (IFN)-γ monoclonal antibody (mAb) (1 mg/ml) for 4 days. The percentages of NKT cells are shown. Data are representative of replicate experiments. (b) The relative increase was based on absolute numbers of NKT cells and was compared with the control expansion culture. Data are shown as mean ± standard deviation for seven independent experiments. A paired two-tailed Student's *t*-test was used for statistical analysis (*$P < 0·01$).

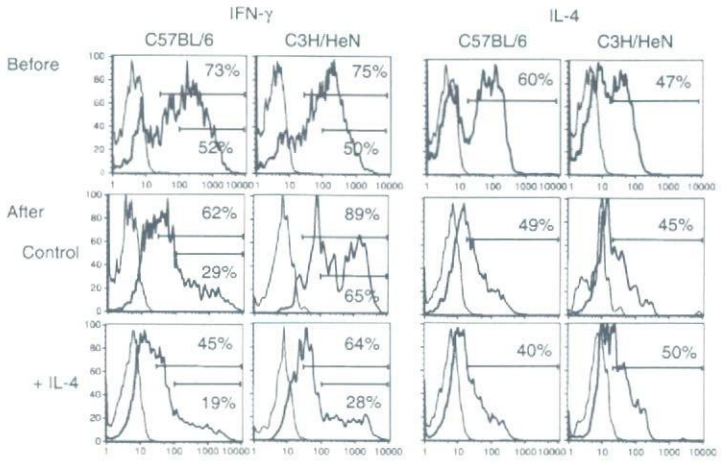


Figure 5. Cytokine production profile of natural killer T (NKT) cells treated with interleukin (IL)-4. Intracellular cytokine staining for interferon (IFN)-γ and IL-4 in NKT cells that were fresh (upper), cultured (middle), or cultured with additional IL-4 (lower) is shown. The cells were stimulated with phorbol 12-myristate 13-acetate (PMA) and ionomycin for 3 hr, stained with anti-CD3 monoclonal antibody (mAb), CD1d/α-galactosylceramide (α-GalCer) tetramer and anti-IFN-γ, anti-IL-4, or an isotype control mAb, and then detected and sorted via flow cytometry. Histogram panels for CD1d/α-GalCer-tetramer$^+$ CD3$^+$ cells are shown. Closed histograms indicate isotype controls. The percentage of total positive and high positive cells are indicated in the histograms. Data are representative of replicate experiments.

whether NKT cells cultured in Th2 conditions produced IFN-γ and IL-4. After 4 days of culture with α-GalCer and IL-2, intracellular IFN-γ- and IL-4-positive NKT cells were observed in both strains of mice. However, the proportion of intracellular IFN-γ high positive NKT cells was reduced when the cells were cultured with additional IL-4 (Fig. 5). In contrast to IFN-γ, the proportion of IL-4-positive NKT cells did not differ between cultures with and without IL-4. Therefore, NKT cells expanding as a result of induction with additional IL-4 displayed a polarized Th2 phenotype.

### NKT cell expansion is accelerated by Th2-biased cytokine conditions

The SJL/J mouse strain is defective in cytokine production by NKT cells, as a consequence of a loss of high-affinity TCR to CD1d, which results from a deletion of the TCR Vβ8 subfamily genomic loci.[28,29] The proportion of NKT cells in the spleens of these mice was lower than that observed for other strains (Fig. 6a), and IFN-γ and IL-4 production after α-GalCer stimulation was also lower than that observed for other strains tested in this study (data not shown). NKT cells from SJL/J mice proliferated even in the absence of additional IL-4, as was observed for NKT cells from C57BL/6 mice. Moreover, similar to findings for NKT cells from C3H/HeN mice, the NKT cell proliferation effect could be enhanced by addition of IL-4 and further enhanced by addition of IL-4 combined with neutralization of IFN-γ (Fig. 6b).

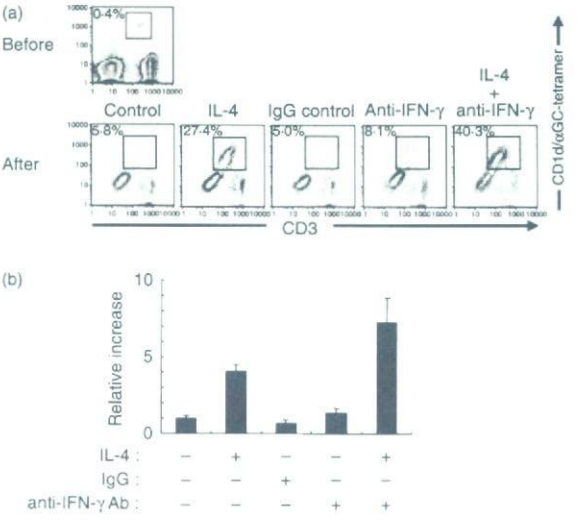


Figure 6. Expansion of natural killer T (NKT) cells from SJL/J mice *in vitro*. (a) Spleen cells ($1 \times 10^6$ cells/ml) were cultured with 50 ng/ml α-galactosylceramide (α-GalCer) and 100 U/ml interleukin (IL)-2 for 4 days with IL-4 (10 ng/ml) and/or anti-interferon (IFN)-γ monoclonal antibody (mAb) (1 mg/ml). The percentages of NKT cells are shown. Data are representative of replicate experiments. (b) The relative increase was based on absolute numbers of NKT cells and was compared with the control expansion culture. Data are shown as the mean of three wells ± standard deviation. Similar results were obtained in two independent experiments.

## Discussion

In a previous study in which we induced expansion of NKT cells collected from human peripheral blood, we


 

observed wide variation in the efficiency of NKT cell expansion.[21] Similarly, when mouse NKT cells were induced to proliferate using similar methods in the present study, the ratios of expanding cell types were distinctly different in cells obtained from different mouse strains (Fig. 1). This suggests that genetic background influences or controls the difference in proliferation efficiency observed in humans and mice. However, we could not rule out the alternative possibility that the effect was a result of bipolar expansion of the cells, rather than originating from genetic variation in one or a few loci.

In this study, we have shown that the amount of IL-4 in the culture supernatant was related to the efficiency of NKT cell expansion induced by α-GalCer and IL-2. Previous studies revealed that addition of exogenous IL-2, IL-7 and IL-15 was able to augment NKT cell expansion by α-GalCer.[30–34] Similarly, in the present study we found that exogenous IL-2 augmented α-GalCer-induced NKT cell expansion in various mouse strains, with the exception of C3H/HeN mice. Moreover, addition of exogenous IL-4 promoted α-GalCer-induced NKT cell expansion in spleen cells from C3H/HeN mice. It has been shown that only NKT cells have the ability to produce IL-4 in this culture.[23] IL-4 might therefore be an autocrine or paracrine growth factor in α-GalCer-induced NKT cell expansion.

NKT cells, NK cells and some T cells when cultured with α-GalCer and IL-2 produce IFN-γ.[23] In contrast to IL-4, the amount of IFN-γ did not correlate with the efficiency of NKT cell expansion. Furthermore, we found that NKT cell proliferation in C3H/HeN mice was slightly increased by neutralization of IFN-γ in the culture. These results suggest that IFN-γ partially inhibits NKT cell expansion by α-GalCer. Interestingly, we found an inverse correlation between the IFN-γ:IL-4 ratio in the culture supernatant after 24 hr of culture and the efficiency of NKT cell proliferation (data not shown). Although higher amounts of IL-4 were detected in the culture of cells from C3H/HeN mice than in the culture of cells from C57BL/6 mice after 24 hr of culture, α-GalCer stimulated spleen cells from C3H/Ne mice produced higher amounts of IFN-γ and exhibited the highest IFN-γ:IL-4 ratio of all mouse strains tested. These results may explain the failure of NKT cell expansion in spleen cells from C3H/HeN mice.

The balance between the production of IFN-γ and the production of IL-4 by NKT cells is influenced by microenvironmental factors such as cytokines and antigen-presenting cells.[20,35–38] IL-7 and IL-12 selectively enhance IL-4 production by NKT cells.[35,36] Antigen-presenting cells such as α-GalCer-pulsed B cells selectively elicit weak IL-4 but not IFN-γ production from NKT cells.[37] There is a high IFN-γ:IL-4 ratio in cultures of spleen cells from C3H/HeN mice, which is caused by splenic NKT cells (A. Iizuka *et al.*, unpublished data) Moreover, it has been reported that the balance of IFN-γ:IL-4 production by NKT cells is developmentally controlled.[39,40] At immature stages, NKT cells predominantly produce IL-4, whereas IFN-γ secretion increases during the course of development.[39] Moreover, immature NKT cells have the ability to proliferate as compared with mature NKT cells.[39] Therefore, NKT cells in the spleen of C3H/HeN mice may be more mature than those of C57BL/6 mice, or contain only a few immature NKT cells. We assume that the failure of proliferation and the high IFN-γ:IL-4 cytokine production ratio of NKT cells in the spleen of C3H/HeN mice were attributable to their maturation stage.

Although IL-4 has opposite effects to IFN-γ and suppresses the Th1 immune response, IL-4 induces proliferation of human IL-13$^+$ NK cells[41] and CD8$^+$ T cells.[42] We found that Th2 culture conditions (in the presence of IL-4 and anti-IFN-γ mAb) facilitated NKT cell expansion induced by α-GalCer and IL-2 even in C3H/HeN and SJL/J mice. IL-4 also induces IFN-γ production by NK and NKT cells *in vivo*.[43] However, the proportion of IFN-γ-positive, but not IL-4-positive, NKT cells decreased when cells were cultured in the presence of IL-4. As in human immature IL-13$^+$ NK cells,[41] IL-4 may induce expansion of developmentally immature NKT cells which have a Th2-biased phenotype.

NKT cell maturation is controlled by the transcription factor T-bet.[44,45] Terminally differentiated NKT cells acquire a strong ability to produce IFN-γ and elicit cytotoxicity.[44] Assuming that expanded Th2-biased NKT cells after culture with α-GalCer, IL-2 and IL-4 are immature cells, it will be possible to induce terminally differentiated Th1-biased NKT cells for Th1 cell immunotherapy, such as cancer cell therapy.

## Acknowledgements

We thank the Pharmaceutical Research Laboratory, Kirin Brewery Co., Ltd (Gunma, Japan) for providing α-GalCer. This work was supported in part by a grant-in-aid for the Third-Term Comprehensive 10-Year Strategy for Cancer Control and for Cancer Research from the Ministry of Health, Labour and Welfare of Japan.

## References

1 Ballas ZK, Rasmussen W. NK1.1$^+$ thymocytes. Adult murine CD4$^-$, CD8$^-$ thymocytes contain an NK1.1$^+$, CD3$^+$, CD5$^{hi}$, CD44$^{hi}$, TCR-Vβ 8$^+$ subset. *J Immunol* 1990; **145**:1039–45.

2 Godfrey DI, Hammond KJ, Poulton LD, Smyth MJ, Baxter AG. NKT cells: facts, functions and fallacies. *Immunol Today* 2000; **21**:573–83.

3 Makino Y, Koseki H, Adachi Y, Akasaka T, Tsuchida K, Taniguchi M. Extrathymic differentiation of a T cell bearing invariant Vα14 Jα281 TCR. *Int Rev Immunol* 1994; **11**:31–46.

4 Gapin L, Matsuda JL, Surh CD, Kronenberg M. NKT cells derive from double-positive thymocytes that are positively selected by CD1d. *Nat Immunol* 2001; **2**:971–8.

5 Mattner J, Debord KL, Ismail N *et al.* Exogenous and endogenous glycolipid antigens activate NKT cells during microbial infections. *Nature* 2005; **434**:525–9.

6 Nishimura T, Santa K, Yahata T *et al.* Involvement of IL-4-producing Vβ 8.2$^+$ CD4$^-$ CD62L$^-$ CD45RB$^-$ T cells in non-MHC gene-controlled predisposition toward skewing into T helper type-2 immunity in BALB/c mice. *J Immunol* 1997; **158**:5698–706.

7 van Der Vliet HJ, Nishi N, de Gruijl TD, von Blomberg BM, van den Eertwegh AJ, Pinedo HM, Giaccone G, Scheper RJ. Human natural killer T cells acquire a memory-activated phenotype before birth. *Blood* 2000; **95**:2440–2.

8 Godfrey DI, Kronenberg M. Going both ways: immune regulation via CD1d-dependent NKT cells. *J Clin Invest* 2004; **114**:1379–88.

9 Arase H, Arase N, Kobayashi Y, Nishimura Y, Yonehara S, Onoe K. Cytotoxicity of fresh NK1.1$^+$ T cell receptor α/β$^+$ thymocytes against a CD4$^+$8$^+$ thymocyte population associated with intact Fas antigen expression on the target. *J Exp Med* 1994; **180**:423–32.

10 Nieda M, Nicol A, Koezuka Y *et al.* TRAIL expression by activated human CD4$^+$Vα24NKT cells induces in vitro and in vivo apoptosis of human acute myeloid leukemia cells. *Blood* 2001; **97**:2067–74.

11 Nicol A, Nieda M, Koezuka Y, Porcelli S, Suzuki K, Tadokoro K, Durrant S, Juji T. Human invariant Vα24$^+$ natural killer T cells activated by α-galactosylceramide (KRN7000) have cytotoxic anti-tumour activity through mechanisms distinct from T cells and natural killer cells. *Immunology* 2000; **99**:229–34.

12 Mattarollo SR, Kenna T, Nieda M, Nicol AJ. Chemotherapy pretreatment sensitizes solid tumor-derived cell lines to Vα24$^+$ NKT cell-mediated cytotoxicity. *Int J Cancer* 2006; **119**:630–7.

13 Smyth MJ, Thia KY, Street SE *et al.* Differential tumor surveillance by natural killer (NK) and NKT cells. *J Exp Med* 2000; **191**:661–8.

14 Seino K, Motohashi S, Fujisawa T, Nakayama T, Taniguchi M. Natural killer T cell-mediated antitumor immune responses and their clinical applications. *Cancer Sci* 2006; **97**:807–12.

15 Metelitsa LS, Naidenko OV, Kant A, Wu HW, Loza MJ, Perussia B, Kronenberg M, Seeger RC. Human NKT cells mediate antitumor cytotoxicity directly by recognizing target cell CD1d with bound ligand or indirectly by producing IL-2 to activate NK cells. *J Immunol* 2001; **167**:3114–22.

16 Giaccone G, Punt CJ, Ando Y *et al.* A phase I study of the natural killer T-cell ligand α-galactosylceramide (KRN7000) in patients with solid tumors. *Clin Cancer Res* 2002; **8**:3702–9.

17 Shimizu K, Hidaka M, Kadowaki N *et al.* Evaluation of the function of human invariant NKT cells from cancer patients using alpha-galactosylceramide-loaded murine dendritic cells. *J Immunol* 2006; **177**:3484–92.

18 Parekh VV, Wilson MT, Olivares-Villagomez D, Singh AK, Wu L, Wang CR, Joyce S, Van Kaer L. Glycolipid antigen induces long-term natural killer T cell anergy in mice. *J Clin Invest* 2005; **115**:2572–83.

19 Ishikawa A, Motohashi S, Ishikawa E *et al.* A phase I study of α-galactosylceramide (KRN7000)-pulsed dendritic cells in patients with advanced and recurrent non-small cell lung cancer. *Clin Cancer Res* 2005; **11**:1910–7.

20 van der Vliet HJ, Molling JW, Nishi N *et al.* Polarization of Vα24$^+$ Vβ11$^+$ natural killer T cells of healthy volunteers and cancer patients using α-galactosylceramide-loaded and environmentally instructed dendritic cells. *Cancer Res* 2003; **63**:4101–6.

21 Harada Y, Imataki O, Heike Y *et al.* Expansion of α-galactosylceramide-stimulated Vα24$^+$ NKT cells cultured in the absence of animal materials. *J Immunother* 2005; **28**:314–21.

22 Kadowaki N, Antonenko S, Ho S, Rissoan MC, Soumelis V, Porcelli SA, Lanier LL, Liu YJ. Distinct cytokine profiles of neonatal natural killer T cells after expansion with subsets of dendritic cells. *J Exp Med* 2001; **193**:1221–6.

23 Ikarashi Y, Iizuka A, Heike Y, Yoshida M, Takaue Y, Wakasugi H. Cytokine production and migration of in vitro-expanded NK1.1$^-$ invariant Vα14 natural killer T (Vα14i NKT) cells using α-galactosylceramide and IL-2. *Immunol Lett* 2005; **101**:160–7.

24 Matsuda JL, Naidenko OV, Gapin L, Nakayama T, Taniguchi M, Wang CR, Koezuka Y, Kronenberg M. Tracking the response of natural killer T cells to a glycolipid antigen using CD1d tetramers. *J Exp Med* 2000; **192**:741–54.

25 Smyth MJ, Crowe NY, Pellicci DG, Kyparissoudis K, Kelly JM, Takeda K, Yagita H, Godfrey DI. Sequential production of interferon-gamma by NK1.1$^+$ T cells and natural killer cells is essential for the antimetastatic effect of α-galactosylceramide. *Blood* 2002; **99**:1259–66.

26 Kambayashi T, Assarsson E, Lukacher AE, Ljunggren HG, Jensen PE. Memory CD8$^+$ T cells provide an early source of IFN-γ. *J Immunol* 2003; **170**:2399–408.

27 Eberl G, MacDonald HR. Rapid death and regeneration of NKT cells in anti-CD3ε- or IL-12-treated mice: a major role for bone marrow in NKT cell homeostasis. *Immunity* 1998; **9**:345–53.

28 Serizawa I, Koezuka Y, Amao H, Saito TR, Takahashi KW. Functional natural killer T cells in experimental mouse strains, including NK1.1$^-$ strains. *Exp Anim* 2000; **49**:171–80.

29 Beutner U, Launois P, Ohteki T, Louis JA, MacDonald HR. Natural killer-like T cells develop in SJL mice despite genetically distinct defects in NK1.1 expression and in inducible interleukin-4 production. *Eur J Immunol* 1997; **27**:928–34.

30 Asada-Mikami R, Heike Y, Harada Y *et al.* Increased expansion of Vα24$^+$ T cells derived from G-CSF-mobilized peripheral blood stem cells as compared to peripheral blood mononuclear cells following α-galactosylceramide stimulation. *Cancer Sci* 2003; **94**:383–8.

31 Imataki O, Heike Y, Ishida T, Takaue Y, Ikarashi Y, Yoshida M, Wakasugi H, Kakizoe T. Efficient ex vivo expansion of Vα24$^+$ NKT cells derived from G-CSF-mobilized blood cells. *J Immunother* 2006; **29**:320–7.

32 Brossay L, Chioda M, Burdin N, Koezuka Y, Casorati G, Dellabona P, Kronenberg M. CD1d-mediated recognition of an α-galactosylceramide by natural killer T cells is highly conserved through mammalian evolution. *J Exp Med* 1998; **188**:1521–8.

33 Nishi N, van der Vliet HJ, Koezuka Y, von Blomberg BM, Scheper RJ, Pinedo HM, Giaccone G. Synergistic effect of KRN7000 with interleukin-15, -7, and -2 on the expansion of human Vα 24$^+$V β11$^+$ T cells *in vitro*. *Hum Immunol* 2000; **60**:357–65.

34 van der Vliet HJ, Nishi N, Koezuka Y *et al.* Potent expansion of human natural killer T cells using α-galactosylceramide

(KRN7000)-loaded monocyte-derived dendritic cells, cultured in the presence of IL-7 and IL-15. *J Immunol Meth* 2001; **247**:61–72.

35 Hameg A, Gouarin C, Gombert JM, Hong S, Van Kaer L, Bach JF, Herbelin A. IL-7 up-regulates IL-4 production by splenic NK1.1$^+$ and NK1.1$^-$ MHC class I-like/CD1-dependent CD4$^+$ T cells. *J Immunol* 1999; **162**:7067–74.

36 Zhu R, Diem S, Araujo LM *et al.* The Pro-Th1 cytokine IL-12 enhances IL-4 production by invariant NKT cells: relevance for T cell-mediated hepatitis. *J Immunol* 2007; **178**:5435–42.

37 Bezbradica JS, Stanic AK, Matsuki N *et al.* Distinct roles of dendritic cells and B cells in Va14Ja18 natural T cell activation in vivo. *J Immunol* 2005; **174**:4696–705.

38 Minami K, Yanagawa Y, Iwabuchi K, Shinohara N, Harabayashi T, Nonomura K, Onoe K. Negative feedback regulation of T helper type 1 (Th1)/Th2 cytokine balance via dendritic cell and natural killer T cell interactions. *Blood* 2005; **106**:1685–93.

39 Benlagha K, Kyin T, Beavis A, Teyton L, Bendelac A. A thymic precursor to the NK T cell lineage. *Science* 2002; **296**:553–5.

40 Pellicci DG, Hammond KJ, Uldrich AP, Baxter AG, Smyth MJ, Godfrey DI. A natural killer T (NKT) cell developmental pathway involving a thymus-dependent NK1.1$^-$CD4$^+$ CD1d-dependent precursor stage. *J Exp Med* 2002; **195**:835–44.

41 Loza MJ, Perussia B. Final steps of natural killer cell maturation: a model for type 1-type 2 differentiation? *Nat Immunol* 2001; **2**:917–24.

42 Ueda N, Kuki H, Kamimura D *et al.* CD1d-restricted NKT cell activation enhanced homeostatic proliferation of CD8$^+$ T cells in a manner dependent on IL-4. *Int Immunol* 2006; **18**:1397–404.

43 Morris SC, Orekhova T, Meadows MJ, Heidorn SM, Yang J, Finkelman FD. IL-4 induces in vivo production of IFN-γ by NK and NKT cells. *J Immunol* 2006; **176**:5299–305.

44 Townsend MJ, Weinmann AS, Matsuda JL, Salomon R, Farnham PJ, Biron CA, Gapin L, Glimcher LH. T-bet regulates the terminal maturation and homeostasis of NK and Vα14i NKT cells. *Immunity* 2004; **20**:477–94.

45 Matsuda JL, Zhang Q, Ndonye R, Richardson SK, Howell AR, Gapin L. T-bet concomitantly controls migration, survival, and effector functions during the development of Vα14i NKT cells. *Blood* 2006; **107**:2797–805.

ANTICANCER RESEARCH *27*: 729-736 (2007)

# Antiproliferating Activity of the Mitotic Inhibitor Pironetin against Vindesine- and Paclitaxel-resistant Human Small Cell Lung Cancer H69 Cells

MITSUZI YOSHIDA[1], YUKI MATSUI[1], YOSHINORI IKARASHI[1], TAKEO USUI[2], HIROYUKI OSADA[2] and HIRO WAKASUGI[1]

[1]*Pharmacology Division, National Cancer Center Research Institute, 5-1-1 Tsukiji Chuo-ku, Tokyo 104-0045;* [2]*Antibiotics Laboratory, RIKEN Discovery Research Institute, 2-1 Hirosawa Wako-shi, Saitama 351-0198, Japan*

**Abstract.** *Pironetin, isolated from Streptomyces sp., is a potent inhibitor of microtubule assembly and the first compound identified that covalently binds to α-tubulin at Lys352. We examined whether pironetin is an effective agent against human small cell lung cancer H69 cells, including two cell lines resistant to the microtubule-targeted drugs vindesine (H69/VDS) and paclitaxel (H69/Txl) that interact with β-tubulin. Pironetin was found to be effective against these resistant cells as well as their parental cells. In addition, pironetin inhibited the growth of human leukemic K562 multidrug-resistant cells (K562/ADM), which have mdr1 gene expression, as well as the parental K562 cells. In these cell lines, including the parental and resistant cells, pironetin caused complete mitotic arrest; in addition, apoptosis inductions by 30 and 100 nM pironetin were observed. In this study, the new mitotic inhibitor, pironetin, was found to be effective not only against human tumor cell lines resistant to microtubule-targeted drugs, but also multidrug-resistant cells with mdr1 gene expression. These results suggest that pironetin is a useful agent for overcoming drug resistance in cancer chemotherapy.*

Microtubules are a cytoskeletal element essential in the segregation of chromosomes during cell division, as well as in axon transport, secretory processes and the maintenance of specific cell morphology. Thus, they are essential in all eukaryotic cells and are among the most successful targets for anticancer chemotherapy. Microtubules are composed of α-tubulin and β-tubulin heterodimers. Microtubule-targeted drugs previously reported have a characteristic ability to bind directly to different sites of β-tubulin *in vitro*. Therefore, they are classified into vinca alkaloid, taxane and colchicine types depending upon their binding site on microtubules.

Pironetin (Figure 1), isolated from *Streptomyces* sp., is a potent inhibitor of microtubule assembly (1) and the first compound identified that covalently binds to α-tubulin at Lys352 (2). In our study, we examined whether pironetin shows antiproliferating activity against clinically employed microtubule-targeted drug-resistant H69 human small cell lung cancer cells and the multidrug-resistant K562 human leukemic cells.

## Materials and Methods

*Chemicals.* Pironetin was kindly supplied from Nippon Kayaku Co., Ltd (Tokyo, Japan). Vindesine sulfate was purchased from Shionogi (Osaka, Japan). Paclitaxel (Taxol®), doxorubicin (Adriamycin®), propidium iodide, Nonidet® p 40, sperminetetrahydrochloride, trypsin, trypsin inhibitor, ribonuclease A, monoclonal anti-P-glycoprotein antibody (Clone F4) and peroxidase-conjugated anti-mouse IgG were purchased from Sigma (St. Louis, MO, USA). Polyclonal anti-caspase-3 antibody was purchased from Cell Signaling Technology (Danvers, MA, USA). Pironetin and paclitaxel were dissolved in dimethyl sulfoxide (DMSO) and used at final concentrations of DMSO below 0.001% and 0.06%, respectively.

*Cell lines.* The human small-cell lung cancer H69 cells and leukemic K562 and HL-60 cells were grown in RPMI-1640 medium supplemented with 10% fetal bovine serum. Vindesine-resistant (H69/VDS) and paclitaxel-resistant (H69/Txl) H69 cells were established in our laboratory as reported elsewhere (3, 4). H69/VDS and H69/Txl resistant cell lines were maintained in the presence of vindesine (10 nM) and paclitaxel (20 nM), respectively, in the culture medium. Doxorubicin-resistant K562 cells (K562/ADM) were used as positive control for typical multidrug-resistant cells expressing the *mdr1* gene (5).

*Correspondence to:* Dr. Mitsuzi Yoshida, Pharmacology Division, National Cancer Center Research Institute, 5-1-1 Tsukiji Chuo-ku, Tokyo 104-0045, Japan. Tel: +81 3 3542-2511, Fax: +81 3 3542-1886, e-mail: myoshida@gan2.res.ncc.go.jp

*Key Words:* Pironetin, mitotic inhibitor, α-tubulin, β-tubulin, resistant cells, vindesine, paclitaxel, *mdr1*, apoptosis, caspase-3, sub-$G_1$.

0250-7005/2007 $2.00+.40

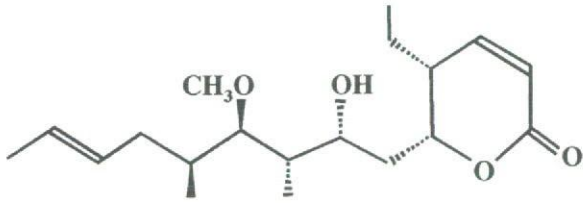


Figure 1. *Chemical structure of pironetin.*

*Antitumor activity in vitro (MTT assay).* Sensitivities of tumor and resistant cell lines to antitumor drugs were examined with a 3-(4,5-dimethyl-2-thiazoyl)-2,5-diphenyltetrazolium bromide (MTT) assay, as outlined elsewhere (6). Briefly, H69/VDS and H69/Txl cells were cultured in vindesine- and paclitaxel-free medium for 1 week before the assay; H69 ($10^4$ cells/ml), H69/VDS ($10^4$ cells/ml), H69/Txl ($2x10^4$ cells/ml), K562 ($2x10^3$ cells/ml), and K562/ADM ($2x10^3$ cells/ml) were then seeded into a 96-well microplate in a volume of 180 μl. A 20-μl aliquot of various concentrations of antitumor drugs was added to each well. Because H69 and its resistant cell lines grow so slowly that their doubling times are over 50 h, differing from the *circa* 12-h doubling time of K562 cell lines, H69 and the resistant cell lines were cultured for 7 days and K562 and its adriamycin-resistant cells were cultured for 4 days at 37°C in an atmosphere of 5% $CO_2$ in air. A 50-μl aliquot of MTT (2 mg/ml) dissolved in $Ca^{2+}$, $Mg^{2+}$-free Dulbecco's phosphate-buffered saline was added to each well and the plates were incubated for 4 h. The MTT-formazan crystals were dissolved in DMSO and the optical density of each solution was measured at 570 nm and 630 nm using a Microplate Manager III (BIO-RAD Laboratories, Hercules, CA, USA) analysis program on a Macintosh computer interfaced with a Benchmark Microplate Reader (BIO-RAD Laboratories).

The $IC_{50}$ was defined as the drug concentration required to inhibit cell growth to 50% that of the control. The relative resistance was defined as the $IC_{50}$ of the resistant subline/$IC_{50}$ of the parental cell line.

*Apoptosis assay (flow cytometry).* Apoptosis induction by pironetin was determined with flow cytometry by the detergent-trypsin method of Vindelov (7). The cells ($5x10^5$) were suspended in 200 μl of citrate buffer including 5% dimethylsulfoxide. Samples were frozen rapidly in polypropylene tubes immersed in a mixture of dry ice and acetone and then stored in a freezer at –80°C. Stock solution: Trisodium citrate (3.4 mM), 0.1% Nonidet® p 40, 1.5 mM sperminetetrahydro-chloride and Tris(hydroxymethyl)-aminomethane were dissolved in distilled water and the pH was adjusted to 7.6. The stock solution was used as the basis for preparing solution A, B and C. Before analysis, the samples were thawed rapidly in a water bath at 37°C and then 1800 μl of solution A (0.003% trypsin in the stock solution) was added to the tube and mixed gently. After 10 min at room temperature, 1500 μl of solution B (0.05% trypsin inhibitor and 0.01% ribonuclease A in the stock solution) were added. The solutions were again mixed by inversion of the tube and after 10 min at room temperature, 1500 μl ice-cold solution C (0.042% propidium iodide and 0.12% spermine tetrahydrocloride in the stock solution) were added. The solutions were mixed for 15 min.

Table I. *Sensitivities of H69, H69/VDS and H69/Txl cells to vindesine, paclitaxel and pironetin in the MTT assay.*

| | $IC_{50}$ (nM) | | |
|---|---|---|---|
| Cell line | Vindesine | Paclitaxel | Pironetin |
| H69 | 5.5±0.3 | 57±1.0 | 17.5±0.9 |
| H69/VDS | 55±4.0 (10.0)* | 530±40 (9.3) | 20.3±2.3 (1.2) |
| H69/Txl | 53±5.0 (9.6) | 2350±260 (41.2) | 11.5±0.4 (0.7) |

*Values in parentheses show relative resistance compared to H69 cells.

The DNA contents were analyzed with the FACSCalibur automated system (BD Biosciences, San Jose, CA, USA) using CellQuest software (BD Biosciences).

*Immunoblot analysis.* Apoptosis caused by pironetin was also detected by immunoblot analysis using polyclonal anti-caspase-3 antibody. Cells were cultured with pironetin and lysed in M-PER mammalian protein extraction reagent (Pierce, Rockford, IL, USA) containing 1 mM dithiothreitol (DTT) and protease inhibitors. Equal amounts of total protein were separated by 4% to 20% (W/V) SDS-PAGE and transferred electrophoretically to polyvinylidene difluoride (PVDF) membranes. Expression of P-glycoprotein in tumor cell lines was also examined by immunoblot analysis using monoclonal anti-P-glycoprotein antibody. Immunoblot stainings were performed as described elsewhere (8).

## Results

*Antiproliferating activity of pironetin against vindesine- and paclitaxel-resistant H69 cells.* Human small cell lung cancer H69 cells were sensitive to vindesine and paclitaxel; the concentration-response curves of H69 to vindesine and paclitaxel obtained are shown in Figure 2. From these figures, the $IC_{50}$s of H69 for vindesine and paclitaxel were estimated as 5.5±0.3 nM and 57±1.0 nM, respectively (Table I). H69/VDS cells resistant to vindesine showed about tenfold resistance to vindesine compared to parental H69 cells. H69/Txl cells showed 41.2-fold resistance to paclitaxel compared to H69 cells. Moreover, at concentrations up to 1 μM, paclitaxel promoted the growth of H69/Txl cells as shown in Figure 2B. H69/Txl and H69/VDS cells were also resistant to vindesine and paclitaxel, with their relative resistances of 9.6 and 9.3, respectively. However, H69/Txl and H69/VDS cells as well as the parental cells were sensitive to pironetin (Figure 3). Pironetin caused growth inhibition of the resistant H69/Txl cells to a higher degree than the parental H69 cells, with a relative resistance of 0.7 (Table I).

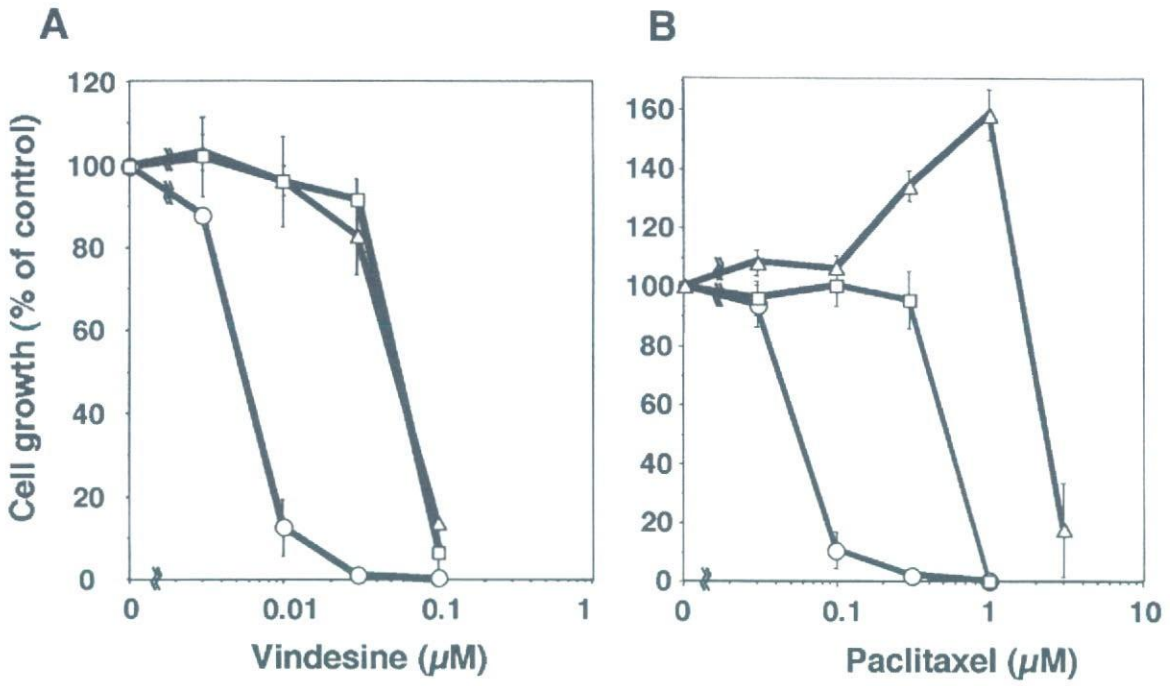


Figure 2. *Concentration-response curves of H69, H69/VDS and H69/Txl cells to (A) vindesine and (B) paclitaxel. Values are average ±S.D. of three independent experiments performed in quintuplicate with H69 (○), H69/VDS (□), and H69/Txl (△) cells. The cells were cultured for 7 days with various concentrations of vindesine or paclitaxel. Cell growth was measured using the MTT assay, as described in Materials and Methods.*

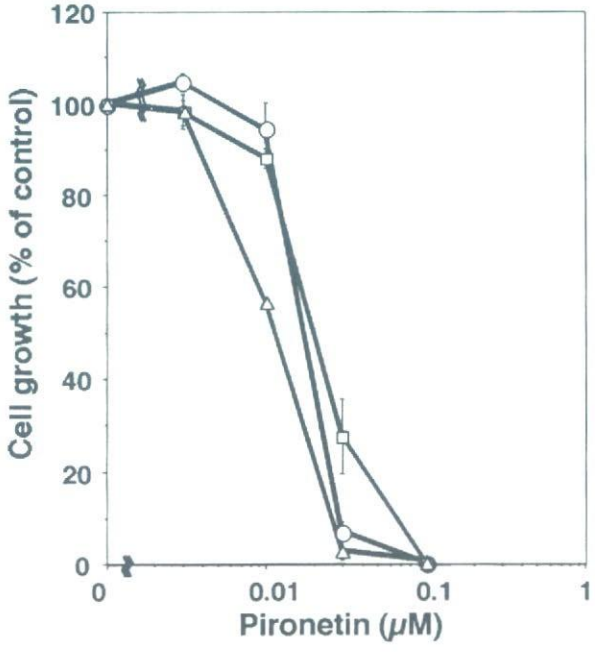


Figure 3. *Concentration-response curves of H69, H69/VDS, and H69/Txl cells to pironetin. Values are average ±S.D. of three independent experiments performed in quintuplicate with H69 (○), H69/VDS (□), and H69/Txl (△) cells. The cells were cultured for 7 days with various concentrations of pironetin. Cell growth was measured using the MTT assay.*

Table II. *Sensitivities of K562 and K562/ADM cells to doxorubicin and pironetin in the MTT assay.*

| Drugs | $IC_{50}$ (nM) | | |
|---|---|---|---|
| | K562 | K562/ADM | Relative resistance |
| Doxorubicin | 52±5.0 | 4500±500 | 86.5 |
| Pironetin | 17.3±0.8 | 16±1.3 | 0.9 |

*Antiproliferating activity of pironetin against K562 and K562/ADM cells.* Figure 4A shows that K562/ADM was strongly resistant to doxorubicin compared to the parental K562 cells. A relative resistance of 86.5 was calculated from this figure (Table II). However, K562/ADM cells showed the same sensitivity to pironetin as the parental K562 cells (Figure 4B). K562/ADM cells are known to be a typical multidrug-resistant cell line that expresses the *mdr1* gene product, P-glycoprotein (Figure 5). Thus, this result suggested that pironetin was not a substrate for P-glycoprotein and that P-glycoprotein did not affect the efflux of pironetin.

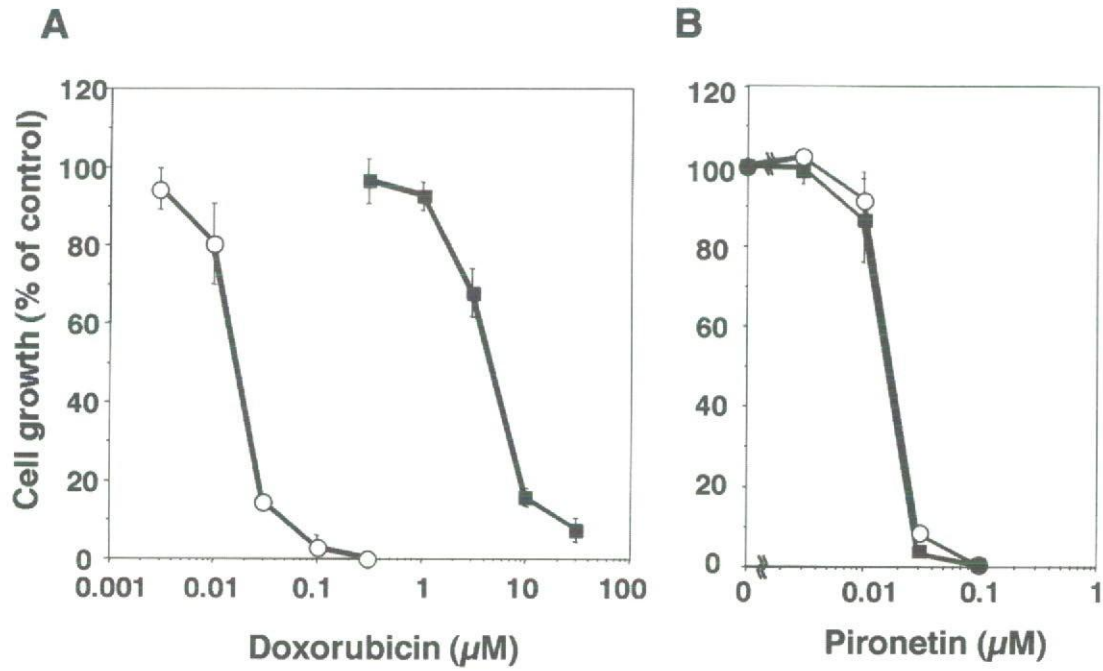


Figure 4. *Concentration-response curves of K562 and K562/ADM cells to (A) doxorubicin and (B) pironetin. Values are average ±S.D. of three independent experiments performed in quintuplicate with K562 (○) and K562/ADM (■) cells. The cells were cultured for 4 days with various concentrations of doxorubicin and pironetin.*

*Apoptosis induction by pironetin.* Pironetin exhibits antitumor activity by apoptosis induction *via* microtubule disassembly (9,10). Therefore, we examined whether apoptosis was similarly induced by pironetin in these resistant cell lines and their parental cell lines. In slow-growing H69 cells, mitotic arrests and sub-$G_1$ peaks in flow cytometric analysis were significantly observed 72 h after pironetin (30 nM) treatment (Figure 6) and signals of cleaved caspase-3 in the immunoblot assay were detected following 30 nM and 100 nM pironetin to the same degree in vindesine- and paclitaxel-resistant cells and the H69 cells (Figure 7). These results suggest that pironetin exhibits antitumor activity against these resistant cell lines *via* apoptosis induction, as in the parental H69 cells.

In human leukemic K562 and doxorubicin-resistant cells (K562/ADM), mitotic arrest and sub-$G_1$ peaks were similarly observed (Figure 8) and signals of cleaved caspase-3 were also detected following 30 nM and 100 nM pironetin treatment (Figure 7). Taken together, pironetin inhibited the growth of vindesine- and paclitaxel-resitant H69 cells to the same degree as in the parental cells, and also the growth of the multidrug-resistant K562 cells as well as parental K562 cells. Using the same concentrations of pironetin (30 nM and 100 nM), apoptosis was induced in these cell lines, although

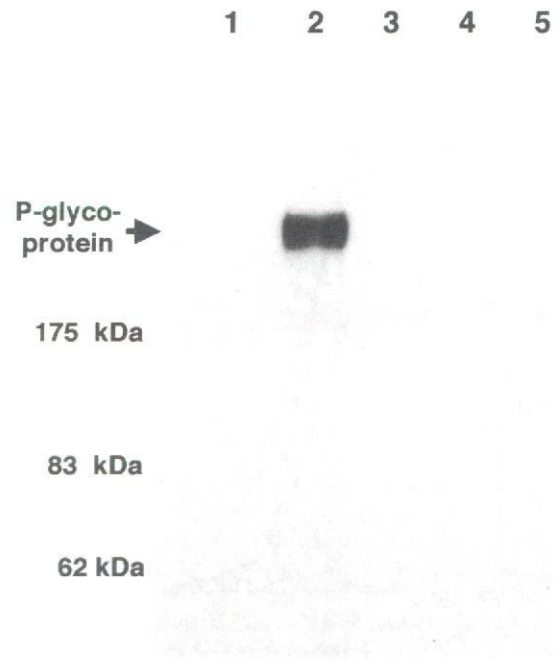


Figure 5. *Western blot analysis of P-glycoprotein. The cell lysates (1 μg) digested by lysis buffer were subjected to 4-20% SDS-PAGE and stained with anti-P-glycoprotein antibody, after being transferred to a PVDF membrane. Lane 1: K562, lane 2: K562/ADM, lane 3: H69, lane 4: H69/VDS and lane 5: H69/Txl.*